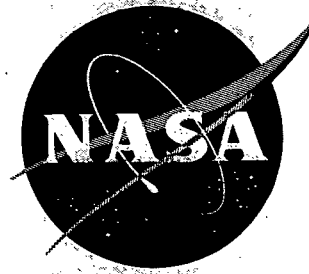


CONFIDENTIAL

62 07dy931 472  
NASA TM X-107

NASA TM X-107



GROUP 4  
Downgraded at 3 year  
intervals; declassified  
after 12 years

# TECHNICAL MEMORANDUM

## X-107

A COMPARISON OF THE PERFORMANCE OF FOUR SIDE-MOUNTED  
INLETS OVER A MACH NUMBER RANGE OF 0.88 TO 2.2  
AND ANGLES OF ATTACK TO 14°

By Leroy L. Presley and William P. Peterson

Ames Research Center  
Moffett Field, Calif.

DECLASSIFIED BY AUTHORITY OF NASA  
CLASSIFICATION CHANGE NOTICES NO. 7  
ITEM NO. 58

SEP 10 1964

CLASSIFICATION - TITLE UNCLASSIFIED

This material contains information affecting the national defense of the United States within the meaning of the espionage laws, Title 18, U.S.C., Secs. 793 and 794, the transmission or revelation of which in any manner to an unauthorized person is prohibited by law.

NATIONAL AERONAUTICS AND SPACE ADMINISTRATION  
WASHINGTON  
January 1960

CONFIDENTIAL

DECLASSIFIED

CONFIDENTIAL

NATIONAL AERONAUTICS AND SPACE ADMINISTRATION

TECHNICAL MEMORANDUM X-107

A COMPARISON OF THE PERFORMANCE OF FOUR SIDE-MOUNTED  
INLETS OVER A MACH NUMBER RANGE OF 0.88 TO 2.2

AND ANGLES OF ATTACK TO  $14^{\circ}$ \*

By Leroy L. Presley and William P. Peterson

SUMMARY

The performance of three external-compression inlets and one internal-compression inlet was investigated experimentally at a Mach number of 2.0 through an angle-of-attack range from  $0^{\circ}$  to  $14^{\circ}$ . The external-compression inlets were as follows: a three-shock vertical-ramp inlet, a two-shock vertical-ramp inlet with a flow-deflector plate, and a three-shock horizontal-ramp inlet. The internal-compression inlet was a circular axisymmetric inlet with a translating centerbody. Each inlet was side-mounted on the forward portion of a 1/10-scale model of a fuselage large enough to accommodate four turbojet engines for operation at Mach number 2.0. Each inlet captured the required air flow for two engines.

Of the four investigated the internal-compression inlet with a flow-deflector plate and the horizontal-ramp inlet had the best pressure-recovery characteristics throughout the entire angle-of-attack range at a Mach number of 2.0. The internal-compression inlet with flow-deflector plate obtained a pressure recovery of 88.3 percent at an angle of attack of  $2^{\circ}$  (zero inlet angle of attack), whereas the horizontal-ramp inlet obtained 87.2 percent. The loss of pressure recovery at positive angles of attack by the vertical-ramp and internal-compression inlets was greatly reduced by a flow-deflector plate mounted above and forward of the inlet entrance.

The drag of the internal-compression inlet with flow-deflector plate was lower than that of any other inlet. The drag of the horizontal-ramp inlet was less than that of the vertical-ramp inlets at angles of attack greater than  $3^{\circ}$ .

---

\*Title, Unclassified

CONFIDENTIAL

CONFIDENTIAL

The horizontal-ramp and internal-compression inlets had suitable pressure-recovery characteristics at Mach numbers below 2.0 but the pressure recovery decreased sharply at Mach numbers above 2.0 at an angle of attack of  $20^\circ$ .

## INTRODUCTION

A large number of studies have been made concerning the performance of side inlets operating at Mach numbers near 2.0. However, most of these studies have dealt with the performance of specific inlet-body combinations which makes a comparison of the relative performance of various types of inlets difficult because of dissimilarities in the flow fields about the various bodies. The present study was initiated, therefore, to compare the pressure recovery and drag of three external-compression inlets and one internal-compression inlet mounted on the side of a given body. The body in this case was a 1/10-scale model of the forward portion of a fuselage large enough to accommodate four turbojet engines for operation at Mach number 2.0. Each of the side inlets supplied the required air flow for two engines.

A  
2  
0  
4

Of the three external-compression inlets, two had vertical compression ramps located on the inboard side of the inlet. (The performance of similar inlets is reported in refs. 1, 2, 3, and 4.) The major difference between the two vertical-ramp inlets was that one incorporated a flow-deflector plate above and forward of the inlet entrance for the intended purpose of improving the performance at angle of attack. The other external-compression inlet had a horizontal compression ramp located at the top of the inlet. (Performance characteristics of a similar inlet are given in ref. 5.)

The internal-compression inlet was axisymmetric and had a translating centerbody. The performance of an isolated inlet of this type has been reported in references 6 and 7, but no data relating to its performance in the presence of a forebody has been published previously. This inlet incorporated flow-deflector plates mounted above and forward of the inlet entrance for improved performance at angle of attack.

Boundary-layer removal was incorporated on the compression surfaces of all the inlets.

The investigation was conducted in the Ames 6- by 6-foot supersonic wind tunnel at a Reynolds number of  $2.5 \times 10^6$  per foot. The Mach number was varied from 0.88 to 2.2 and data were obtained for model angles of attack from  $0^\circ$  to  $14^\circ$ .

CONFIDENTIAL

DECLASSIFIED

CONFIDENTIAL

3

# SYMBOLS

A	cross-sectional area, sq in.
$C_D$	total drag coefficient based on maximum body cross-sectional area
$c_d$	internal drag of bleed systems
H.R.P.	horizontal reference plane
m	mass-flow rate of air, slugs/sec
M	Mach number
p	static pressure, lb/sq in.
$\frac{\Delta p_t}{p_{t_{av}}}$	total-pressure distortion parameter, numerical difference between maximum and minimum rake total pressures divided by average total pressure
$\alpha$	angle of attack, deg
$\delta$	second-ramp angle, deg

# Subscripts

b	total bleed
i	inlet entrance
l	local value
L	left duct, viewed from rear
R	right duct, viewed from rear
t	stagnation condition
av	average
max	maximum
min	minimum

CONFIDENTIAL

4

- ∞ free stream
- 1 compressor rake station
- 2 ramp bleed mass-flow measuring station for vertical-ramp inlets
- 3 mass-flow measuring station for horizontal-ramp inlet bleed through ramp perforations
- 4 mass-flow measuring station for horizontal-ramp inlet bleed through ramp slot
- 5 mass-flow measuring station for internal-compression inlet centerbody bleed
- 6 mass-flow measuring station for internal-compression inlet annulus bleed
- 7 mass-flow measuring station for gutter bypass air
- 8 mass-flow measuring station for upper bypass of engine air
- 9 mass-flow measuring station for lower bypass of engine air

## APPARATUS AND PROCEDURE

### Model

The model investigated represented to a scale of 1 to 10 the forward portion of a fuselage sized to accommodate four turbojet engines for operation at Mach number 2. The model had two side-mounted inlets, each supplying air to two of the four turbojet engines. In the present tests, however, the right inlet was faired over. All of the inlets tested were separated from the fuselage by a boundary-layer diverter of sufficient height to insure that none of the low-energy boundary-layer air entered the inlet. At the nose of the diverter, a scoop was incorporated to capture a mass of air approximately equal to 2 percent of the inlet mass flow. All of the inlets were canted downward  $2^\circ$  with respect to the horizontal reference plane of the fuselage. Photographs and schematic diagrams of the model are shown in figures 1 through 8.

The internal ducting of the model is shown schematically in figure 3. From the inlet entrance the air flowed in a single duct until it was divided into two ducts at station 62.17. From this point, the air flowed past the simulated engine compressor station and out the exit in two separate channels. A movable throttling plug at the exit controlled the

mass flow through each duct. At station 55.98 air could be removed from the single duct to simulate the engine air bypass that would be required to match the main air supply with that demanded by the engines. Besides the diverter scoop and the main duct bypass systems, a system was provided to remove boundary-layer air from the compression surfaces of each of the inlets. All auxiliary ducts discharged in the same plane as the main inlet ducts but no control over their mass flow was provided.

### Inlet Details

Four separate inlets were investigated; a three-shock vertical-ramp inlet (basic inlet), a two-shock vertical-ramp inlet with a flow deflector plate (hooded inlet), a three-shock horizontal-ramp inlet, and a circular internal-compression inlet. Photographs of the four inlet models are shown in figure 4. Details of the four inlets are given in figures 5, 6, 7, and 8. Boundary-layer transition wires were attached to the model (see figs. 1, 2, and 4) to insure that the transition point of the boundary layer would be fixed. The size of the wire, 0.02-inch diameter, was determined from reference 8.

Three-shock vertical-ramp inlet (basic inlet) (figs. 4(a) and 5).— The three-shock vertical-ramp inlet, referred to hereafter as the basic inlet, had a short first ramp, fixed at an angle of  $6^\circ$  with respect to the inlet center line, and a variable second ramp, which for this test was set at an angle of  $12^\circ$  with respect to the first ramp. The short first ramp was used to provide a hinge fairing rather than a two-shock compression ramp. The internal area distribution is shown in figure 9. Boundary-layer air could be removed from the surface of the second ramp through holes drilled perpendicular to the surface.

Two-shock vertical-ramp inlet (hooded inlet) (figs. 4(b) and 6).— The two-shock vertical-ramp inlet, referred to as the hooded inlet, differed from the basic inlet in that a flow-deflector plate was placed in line with the top of the inlet to improve the performance at angle of attack. As a result of adding the flow-deflector plate, the short first compression ramp was replaced by a long splitter plate. This left only one compression ramp which for this test was set at an angle of  $18^\circ$  with respect to the inlet center line. The internal area distribution of this inlet is shown in figure 9. The boundary-layer-removal system was the same as for the basic inlet.

Three-shock horizontal-ramp inlet (figs. 4(c) and 7).— The three-shock horizontal-ramp inlet, referred to as the horizontal-ramp inlet, had a fixed first-ramp angle of  $6^\circ$  with respect to the horizontal reference plane and a variable second-ramp angle. The second-ramp angle was varied by inserting ramps of fixed angle ( $0^\circ$ ,  $6^\circ$ ,  $9^\circ$ , and  $12^\circ$  with respect to the first ramp) into the inlet. The inlet also incorporated

031712281030

CONFIDENTIAL

a removable side fairing on the inboard edge, as shown by the dotted line at the front of the vertical section in figure 7. The internal area distributions of the inlet are shown in figure 10.

The four boundary-layer-removal configurations investigated on this inlet consisted of perforated surfaces and flush full-width slots in the second-ramp surface (for details see fig. 7(b)). The air from the porous section was exhausted overboard through a converging-diverging nozzle at an average angle of  $27\text{-}1/2^\circ$  with respect to the inlet center line, while the air from the slot was exhausted through the boundary-layer-removal duct.

Circular internal-compression inlet (figs. 4(d) and 8).- The circular internal-compression inlet, referred to as the internal-compression inlet, had a centerbody which could be translated forward and rearward to vary the internal area distribution as shown in figure 11. With the centerbody fully retracted the contraction ratio  $A_{\min}/A_1$  was 0.65. Other design and operation principles for this type of inlet are discussed in references 6 and 7.

Boundary-layer air was removed from both the annulus and centerbody surfaces. The air removed from the annulus surface was exhausted overboard through a converging-diverging nozzle at an average angle of  $27\text{-}1/2^\circ$  with respect to the inlet center line. The holes in the annulus employed simple check valves to allow the air to flow in only one direction (see fig. 8(a)). Figure 8(b) shows the three boundary-layer-removal configurations that were used on the centerbody. They were (1) seven rows of holes drilled perpendicular to the centerbody center line, (2) a flush slot, and (3) a forward facing scoop. In each configuration the air traveled down the centerbody sting, through the cruciform supports and out the boundary-layer-removal duct (see fig. 3). The relative position of the various boundary-layer-removal systems for various centerbody positions is shown on the area distribution curves in figure 11.

To improve the performance of the inlet at angle of attack, four flow-diverter plates were tested as shown in figure 8(c). The plates were located above and ahead of the inlet entrance and were designed so that at  $M_\infty = 2.0$  and with the inlet at  $0^\circ$  angle of attack the Mach lines emanating from the plate leading edge enveloped most of the inlet entrance. (The focal point of the Mach lines was assumed to lie on a line through the center of curvature of the plates.) The height of the gap between the bottom surface of the plate and the top of the inlet was made 0.25 inch to prevent the boundary layer of the plate from entering the inlet.

CONFIDENTIAL

DECLASSIFIED

CONFIDENTIAL

7

## Instrumentation

The model was sting mounted in the tunnel and the normal and chordwise forces acting on the forebody were measured with a strain-gage balance. The shroud and throttling plug mechanism were mounted on the sting and therefore did not affect the forces indicated by the balance. The shroud was cantilevered forward over the afterbody to prevent air from impinging on the model base and ducting except for the amount that could pass through the small gap between the body and shroud at the shroud junction.

The following instrumentation was used to measure steady-state pressures: a boundary-layer survey rake (located at station 30.57) was mounted on the right side of the fuselage ahead of the closed dummy inlet; static and total-pressure rakes (shown in fig. 12) were located at station 66.67 (simulated engine compressor station) and 86.97 in each of the two main ducts; a static orifice and a total pressure tube were located in each of the auxiliary ducts at station 85.17 and in the case of the horizontal-ramp inlet and internal-compression inlet, static-pressure orifices and total-pressure rakes were placed in the boundary-layer-removal exhaust nozzles. The base pressure on the forebody was measured by static-pressure orifices located around the base area.

All pressure tubes were connected to mercury-fluid multimanometers and the manometer readings were recorded photographically. In the case of the main duct rakes located at stations 66.67 and 86.97 integrating pressure cells were used in conjunction with automatic recording and computing equipment to obtain average values of the static and total pressures.

A bonded strain-gage pressure transducer for sensing dynamic pressure fluctuations was placed in the model at station 65.17. This transducer was mounted with its diaphragm flush with the wall of the duct and had a resonant frequency of 5000 cycles per second. The output signal from the transducer was recorded on magnetic tape.

## Data Reduction

The total pressure in each duct at the simulated compressor station was based on an area-weighted average of the 30 total-pressure readings at station 66.67. The average total-pressure recovery of the inlet was computed as the arithmetic average of the pressure recoveries in the two main ducts.

The mass-flow ratio of the main ducts was found from the continuity equation using values of  $p/p_t$  and  $p_t$  measured at the exit rake at

CONFIDENTIAL



03170001030

CONFIDENTIAL

station 86.97 and a calibration factor determined during the test. The exit rake was used because it indicated near pipe flow velocity profiles in the ducts for all test conditions. The calibration factor was found by operating the internal-compression inlet supercritically. (For this condition the inlet captures a stream tube equal in area to the inlet entrance area, thus insuring a mass-flow ratio of unity. The total-pressure loss at the model nose was not accounted for however.) The mass-flow ratios of the auxiliary ducts and exhaust nozzles were determined from measured values of  $p/p_t$  and  $p_t$  and a calibration factor obtained from static bench tests.

The internal momentum loss of the main duct flow was subtracted from the net drag force to obtain the external drag of the model. The losses of the boundary-layer-removal systems and gutter-bleed system were charged against the inlet system by not correcting the force measurements for their momentum losses.

The dynamic pressure fluctuations which were recorded on magnetic tape during the test were analyzed on a spectrum analyzer. From this analysis the root mean pressure fluctuations and predominant frequency of the oscillations were obtained.

## RESULTS AND DISCUSSION

All the data obtained in this investigation are presented in tabular form in table I. Some of these data have been summarized in figures 13 to 22 for discussion purposes. The major portion of the discussion is devoted to the performance of the four inlets at  $M_\infty = 2.0$  through the angle-of-attack range of  $0^\circ$  to  $14^\circ$ . The performance of the horizontal-ramp and internal-compression inlets at Mach numbers ranging from 0.88 to 2.2 at an angle of attack of  $2^\circ$  will also be discussed.

### Performance at $M_\infty = 2.0$

Pressure recovery.— The pressure recovery of an inlet which is mounted on the side of a fuselage is dependent upon the properties of the flow field around the forebody. This forebody has two primary effects upon the flow field at the inlet entrance. First, at supersonic speeds, the available energy is decreased because of the presence of the shock wave at the model nose. Secondly, a boundary layer is built up along the forebody which represents an additional loss in total pressure. To overcome the second adverse effect, all of the inlets were separated from the side of the fuselage by a boundary-layer diverter, as discussed previously. It was confirmed from the boundary-layer profiles shown in figure 13 and schlieren observations that the extreme low-energy portions of the boundary

CONFIDENTIAL

DECLASSIFIED

CONFIDENTIAL

9

layer did not enter any of the inlets. The loss in total pressure due to the forebody is also shown in figure 13 and is seen to be from 3 to 6 percent outside of the boundary layer for the entire angle-of-attack range investigated.

The best total-pressure recovery obtained by each of the four inlets is summarized in figure 14 and is discussed in detail in the following paragraphs.

Basic inlet: The basic inlet obtained a maximum pressure recovery of 82.8 percent at an airplane angle of attack of  $2^\circ$  which corresponds to zero inlet angle of attack. This pressure recovery is low compared to that of other three-shock vertical-ramp inlets (refs. 1, 2, and 3) and can be attributed to the design shock structure. The relative locations of the first and second ramps were such that the two oblique shocks generated by these two ramps intersected only a short distance from the ramp surfaces. This had the effect of giving the inlet operating characteristics that would be more closely associated with a single-ramp inlet having a deflection angle of  $18^\circ$  ( $6^\circ$  first ramp and  $12^\circ$  second ramp).

The basic inlet is seen to be fairly insensitive to variations of angle of attack to  $6^\circ$  in that the pressure recovery was within 1 percent of the value at  $2^\circ$  angle of attack. However, above  $\alpha = 6^\circ$ , the pressure recovery decreased sharply to a value of 67 percent at  $14^\circ$  angle of attack. This variation of pressure recovery with angle of attack is typical for inlets of this type in this speed range (see refs. 1, 2, and 3).

Hooded inlet: The hooded inlet, because of similarities in shock structure and internal contours, was expected to obtain a pressure recovery near that of the basic inlet but fell far short, obtaining a pressure recovery of only 70.3 percent at an angle of attack of  $2^\circ$  (see fig. 14). The poor pressure recovery of the hooded inlet is believed to be due to interaction of the shock wave of the compression ramp and the boundary layer of the splitter plate. Also, since no provision was made to prevent the boundary layer of the flow-deflector plate from entering the inlet, the oblique and normal shocks of the compression process would probably interact unfavorably with the boundary layer of the flow-deflector plate.

The characteristics at angle of attack of the hooded inlet were, however, favorable. The pressure recovery increased from 70.3 percent at  $\alpha = 2^\circ$  to 80.8 percent at  $\alpha = 10^\circ$ . These results indicate that the horizontal-flow deflector plate is effective in improving the performance at angle of attack of an inlet of this type. The sharp decrease in pressure recovery above an angle of attack of  $10^\circ$  is due to detachment of the oblique shock wave from the compression ramp.

Horizontal-ramp inlet: The horizontal-ramp inlet operating with bleed system No. 1 (shown in fig. 7(b)) and the sharply swept side

CONFIDENTIAL

A-204

CONFIDENTIAL

splitter plate,<sup>1</sup> obtained a maximum pressure recovery of 84.4 percent at an angle of attack of  $2^\circ$  (see fig. 14). This value was believed to be considerably below the potential of the inlet since the pressure recovery from the shock structure alone would be near 96 percent. Therefore a secondary investigation was conducted to determine the effect of variations in the bleed system upon the pressure recovery of the inlet. The first step was to decrease the amount of air removed from the forward part of the second ramp since it was speculated that removal of air at this location could have the effect of decreasing the turning angle felt by the air and thus decreasing the pressure recovery. The results of this investigation are shown in figure 15. It is seen that decreasing the mass flow through the forward opening from 1.1 percent of the inlet mass flow (bleed system No. 1) to 0.4 percent (bleed system No. 2), to 0 (bleed system No. 3), by decreasing the number of holes as shown in figure 7(b), increased the peak pressure recovery from 84.4 to 87 to 87.2 percent. (The mass flow through the rear slot was held constant at 2.2 percent of the inlet mass flow while this was being done.) The mass flow through the rear slot was then increased to 3 percent (bleed system No. 4), by widening the slot (see fig. 7(b) and ref. 9) with the forward bleed sealed, with the result that the pressure recovery was decreased from 87.2 percent to 84.8 percent. From the data obtained, it appears that there is an optimum bleed configuration. Bleed on the forward ramps has the effect of decreasing the effective ramp angle while too much bleed in the throat decreased the effective internal contraction.

A  
2  
0  
4

For the operation of a horizontal-ramp inlet at positive angles of attack, the second ramp deflection angle must be varied to obtain a shock structure conducive to high pressure recovery. The pressure recovery with bleed system No. 1 for various second-ramp deflection angles is shown in figure 16 as a function of angle of attack. The operating envelope for the angle-of-attack range would entail a schedule of the second-ramp deflection angle that would yield maximum pressure recovery at any given angle of attack. Such an operating envelope for this inlet is shown in figure 14. The highest pressure recovery of 87.9 percent was obtained at an angle of attack of  $4^\circ$  where, as shown in reference 10, the combination of ramp deflection angles is nearest the theoretical optimum for a Mach number of 2.0. The variation in pressure recovery throughout the entire angle-of-attack range is seen to be within  $\pm 5$  percent of the value at  $2^\circ$  angle of attack, thus making this inlet attractive from the standpoint of high-pressure-recovery characteristics at angle of attack.

Internal-compression inlet: The internal-compression inlet obtained a maximum pressure recovery of 88.3 percent at  $2^\circ$  angle of attack (see

<sup>1</sup>Tests were also conducted with a less swept side splitter plate similar to that used with the hooded inlet. Data from these tests are not presented because there was essentially no effect on side-plate sweep on pressure recovery for the horizontal-ramp inlet.

CONFIDENTIAL

DECLASSIFIED

CONFIDENTIAL

11

fig. 14) with a bleed system consisting of a ram scoop on the centerbody and 9 rows of holes on the annulus (see figs. 8(a) and (b)). The pressure recovery obtained with various bleed systems on the centerbody with an identical annulus bleed system is shown in figure 17. The lack of any significant difference in the pressure recovery obtained by the various bleed systems is believed to be due to the limited mass flow that could be removed through the centerbody support sting.

The pressure recovery of the internal-compression inlet was found to be very sensitive to changes in angle of attack as shown in figure 18. However, figure 18 also shows that the addition of a flow-deflector plate above and forward of the inlet entrance is an effective method of improving the pressure recovery at angle of attack of this type of inlet (see also ref. 7). The best pressure recovery was obtained with the sharply downward curved flow-deflector plate (fig. 8(c), plate No. 1), and these data were used in the inlet comparison shown in figure 14. The pressure recovery with this plate varied only -5 percent from the  $\alpha = 2^\circ$  value for the entire angle-of-attack range. Since all of the configurations should obtain the same pressure recovery at  $2^\circ$  angle of attack, the scatter shown is to a certain extent an indication of the repeatability of data for this inlet.

From the previous discussion, it can be seen that the internal-compression inlet with a flow-deflector plate and the horizontal-ramp inlet had good pressure-recovery characteristics throughout the entire angle-of-attack range. The flow-deflector plates on the internal-compression inlet and on the vertical-ramp inlet were found to be effective in improving the performance of inlets which were otherwise sensitive to angle of attack.

Total-pressure distortion.- The total-pressure distortion parameter,  $(\Delta p_t / p_{t_{av}})$  (shown in fig. 19), at the body station corresponding to the entrance to the jet engine compressor was less than 0.13 for all inlets for the pressure recoveries shown in figure 14. The variation of distortion with angle of attack is seen to be erratic for all of the inlets with little evidence of any general trends. The difference in distortion between the two ducts is seen to be small.

Total drag.- The total drag coefficients of the four inlet-body combinations for the pressure recoveries shown in figure 14 are given in figure 20 as functions of angle of attack. Comparisons of the drag of the various inlets can best be seen in figure 21 where the difference in drag coefficient of each inlet from that of the basic inlet is given as a function of angle of attack. It should be mentioned that the drag of the basic inlet is high because of a large spillage drag. This occurred because the inlet operated at critical mass-flow ratios less than 0.80 as a result of its having internal contraction in excess of the maximum allowable for starting.

CONFIDENTIAL

CONFIDENTIAL

The hooded inlet had a lower drag coefficient than the basic inlet for angles of attack up to  $7^\circ$  but became greater at angles of attack above  $7^\circ$ . The difference in drag between this inlet and the basic inlet is due to differences in wave and spillage drag.

The drag coefficient of the horizontal-ramp inlet was comparable to that of the basic inlet at angles of attack of  $0^\circ$  and  $2^\circ$ , but less than that of the basic inlet at angles of attack above  $2^\circ$ . This inlet had higher wave drag than the basic inlet, thus indicating that the decrease in drag with angle of attack was due to the reduction of the spillage drag.

Of the inlets considered in figure 20 the drag coefficient of the internal-compression inlet with flow deflector is seen to be the lowest throughout the angle-of-attack range. The drag of this inlet without the flow-deflector plate up to angles of attack of approximately  $8^\circ$  is purely due to friction and wave drag since the inlet was operating at mass-flow ratio of unity. The increment of wave drag due to the addition of the flow-deflector plate was from 5 to 10 percent over that of the inlet alone (see tabulated data).

Inlet instability.- A comprehensive and systematic investigation of inlet instability was believed to be beyond the scope of this investigation, although data were taken at typical points where instability occurred. These operating conditions usually occurred when the external-compression inlets were operating at low mass-flow ratios ( $m/m_\infty \approx 0.5$ ) or when the internal-compression inlet had regurgitated the terminal shock and the centerbody was being translated forward to start the inlet. Typical values of the root mean square of the static-pressure fluctuations associated with instability were  $0.044 p_{t_\infty}$  for the basic inlet,  $0.128 p_{t_\infty}$  for the hooded and horizontal-ramp inlets, and  $0.115 p_{t_\infty}$  for the internal-compression inlet. The peak pressure fluctuations occurred at a predominant frequency between 40 and 43 cycles per second for the external-compression inlets and near 32 cps for the internal-compression inlet. These data were taken at  $\alpha = 2^\circ$ , and were measured at station 65.17.

#### Off-Design Characteristics

Only the horizontal ramp and the internal-compression inlets were tested at Mach number other than 2.0 ( $0.88 \leq M_\infty \leq 2.2$ ). The pressure recoveries obtained with these inlets are shown in figure 22 for an angle of attack of  $2^\circ$ .

The horizontal-ramp inlet yields suitable performance at Mach numbers of 2.0, 1.60, and 0.88 by decreasing the second-ramp angle from  $12^\circ$  to  $6^\circ$  to  $0^\circ$ , respectively. The pressure recovery decreased at a Mach number

CONFIDENTIAL

DECLASSIFIED

CONFIDENTIAL

13

of 2.2 since the maximum second ramp deflection angle was  $12^\circ$  which is too low for this Mach number.

The pressure recovery of the internal-compression inlet with flow deflector plate No. 4 was satisfactory at Mach numbers of 2.0, 1.85, and 0.88. For suitable performance at Mach numbers below 2.0, the center-body of the internal-compression inlet must be translated forward to obtain contraction ratios which are compatible with the lower Mach numbers. The pressure recovery decreased at Mach numbers above 2.0 since the inlet reached its maximum contraction ratio near  $M_\infty = 2.05$ , thus no further internal contour changes could be made.

#### SUMMARY OF RESULTS

The performance of three external-compression and one internal-compression inlets was investigated at a Mach number of 2.0 and angles of attack to  $14^\circ$ . The performance of the internal-compression and of one of the external-compression inlets (three-shock horizontal-ramp inlet) was investigated at Mach numbers from 0.88 to 2.2 at an angle of attack of  $2^\circ$ . Each inlet was mounted individually on the side of a common fuselage. The results of the investigation were as follows:

1. Of all the inlets tested at a Mach number of 2, the internal-compression inlet obtained the highest pressure recovery at an angle of attack of  $2^\circ$ . This inlet with a flow-deflector plate also obtained the highest pressure recovery of all the inlets throughout the entire angle-of-attack range. Of the external-compression inlets tested, the horizontal-ramp inlet had the highest pressure recovery.

2. For all the inlets tested, the total-pressure distortion at the compressor rake station was less than 12 percent throughout the entire angle-of-attack range at a Mach number of 2.0. The difference in distortion between the two engine ducts which were supplied by one inlet was generally low.

3. The drag of the internal-compression inlet with flow-deflector plate was the lowest of all the inlets tested at a Mach number of 2.0. The drag of the horizontal-ramp inlet was less than that of the two vertical-ramp inlets at angles of attack greater than  $3^\circ$ .

CONFIDENTIAL

03:17:00 10:30

14

~~CONFIDENTIAL~~

4. The pressure recovery of both the internal-compression and horizontal-ramp inlets, which were  $M = 2.0$  designs, remained high at Mach numbers less than 2.0, but decreased sharply at Mach numbers greater than 2.0.

Ames Research Center

National Aeronautics and Space Administration

Moffett Field, Calif., Aug. 11, 1959

#### REFERENCES

1. Obery, Leonard J., Stitt, Leonard E., and Wise, George A.: Evaluation at Supersonic Speeds of Twin-Duct Side-Intake System With Two-Dimensional Double-Shock Inlets. NACA RM E54C08, 1954.
2. Stitt, Leonard E., and Wise, George A.: Investigation of Several Double-Ramp Side Inlets. NACA RM E54D20, 1954.
3. Yeager, Richard A., Beheim, Milton A., and Klann, John L.: Performance of Twin-Duct Variable-Geometry Side Inlets at Mach Numbers of 1.5 and 2.0. NACA RM E56K15, 1957.
4. Allen, John L.: Performance of a Blunt-Lip Side Inlet With Ramp Bleed, Bypass, and a Long Constant-Area Duct Ahead of the Engine: Mach Numbers 0.66 and 1.5 to 2.1. NACA RM E56J01, 1956.
5. Wise, G. A., and Campbell, R. C.: Investigation of a Ramp-Type Inlet Designed for Improved Angle-Of-Attack Performance at Mach Number 2.0. NACA RM E54L17, 1955.
6. Mossman, Emmet A., and Pfyl, Frank A.: An Experimental Investigation at Mach Numbers From 2.1 to 3.0 of Circular-Internal-Contraction Inlets With Translating Centerbodies. NACA RM A56G06, 1956.
7. Pfyl, Frank A., and Watson, Earl C.: An Experimental Investigation of Circular Internal-Compression Inlets With Translating Centerbodies Employing Boundary-Layer Removal at Mach Numbers From 0.85 to 3.50. NASA MEMO 2-19-59A, 1959.
8. Winter, K. G., Scott-Wilson, J. B., and Davies, F. V.: Methods of Determination and of Fixing Boundary Layer Transition on Wind Tunnel Models at Supersonic Speeds. British R.A.E. TN Aero. 2341, Sept. 1954.

~~CONFIDENTIAL~~

DECLASSIFIED

CONFIDENTIAL

15

~~CONFIDENTIAL~~

9. Vargo, Donald J., Parks, Philip N., and Davis, Owen H.: Investigation of a High-Performance Top Inlet to Mach Number of 2.0 and at Angles Of Attack to  $20^{\circ}$ . NACA RM E57A21, 1957.
10. Connors, James F., and Meyer, Rudolph C.: Design Criteria for Axisymmetric and Two-Dimensional Supersonic Inlets and Exits. NACA TN 3589, 1956.

CONFIDENTIAL



CONFIDENTIAL

CONFIDENTIAL

TABLE I.- PERFORMANCE OF INLET CONFIGURATIONS  
(a) Three-shock vertical ramp inlet (basic inlet)

$M_\infty$	$\alpha$ , deg	$\left(\frac{m_1}{m_\infty}\right)_L$	$\left(\frac{m_1}{m_\infty}\right)_R$	$\left(\frac{P_{t1}}{P_{t_\infty}}\right)_L$	$\left(\frac{P_{t1}}{P_{t_\infty}}\right)_R$	$\left(\frac{P_{t1}}{P_{t_\infty}}\right)_L$	$\left(\frac{P_{t1}}{P_{t_\infty}}\right)_R$	$C_D$	$\frac{W}{W_\infty}$	$\frac{m}{m_\infty}$	$c_{d1}$	$c_{d2}$
2.029	0	0.4345	0.4201	---	0.7691	0.10071	0.1436	0.1381	0.011	0.019	0.0018	0.0036
		.4298	.4121	0.8195	.7975	.0927	.0927	.1378	.010	.019	.0018	.0036
		.3881	.3774	.8291	.8053	.0518	.0626	.1427	.010	.023	.0018	.0039
		.3588	.3532	.8224	.8004	.0316	.0400	.1522	.010	.028	.0018	.0040
		.3284	.3334	.8178	.7975	.0244	.0276	.1609	.010	.030	.0018	.0041
2.018	2.02	.3125	.3107	.7921	.7806	.0328	.0288	.1638	.010	.031	.0017	.0041
		.4563	.4284	.7972	.7543	.1423	.1332	.1341	.011	.017	.0017	.0032
		.4398	.4260	.8005	.7510	---	---	.1357	.010	.017	.0018	.0035
		.4285	.4224	.8207	.8020	.1077	.0990	.1406	.009	.021	.0018	.0038
		.4067	.4058	.8329	.8156	.0726	.0796	.1442	.009	.024	.0018	.0039
2.026	6.01	.3812	.3898	.8342	.8201	.0587	.0682	.1513	.009	.025	.0018	.0040
		.3578	.3627	.8291	.8185	.0373	.0480	.1503	.009	.029	.0018	.0041
		.2910	.2985	.8207	.8168	.0243	.0239	.1782	.010	.034	.0018	.0041
		.2521	.2676	.8086	.8066	.0216	.0192	.1903	.010	.038	.0018	.0041
		.2026	.2189	.8009	.7975	.0218	.0188	.2048	.010	.038	.0018	.0040
2.025	10.00	.4366	.4319	.8161	.7991	.1106	.1007	.1398	.010	.022	.0018	.0038
		.4434	.4181	.7875	.7382	.1986	.1476	.1904	.011	.017	.0019	.0035
		.4457	.4136	.8308	.7757	.1413	.1108	.1917	.011	.017	.0019	.0036
		.4126	.3990	.8321	.7917	.0798	.0845	.1969	.012	.022	.0019	.0039
		.3923	.3735	.8426	.8037	.0486	.0625	.2042	.011	.025	.0019	.0041
2.024	13.99	.3585	.3534	.8413	.8107	.0350	.0386	.2126	.011	.028	.0019	.0041
		.3275	.3301	.8346	.8107	.0293	.0308	.2213	.011	.030	.0019	.0042
		.2786	.2856	.7938	.7806	.0440	.0345	.2327	.011	.031	.0019	.0042
		.4101	.3587	.7333	.6406	.1403	.1037	.3128	.011	.019	.0019	.0037
		.4079	.3752	.7694	.6907	.1045	.0846	.3130	.011	.020	.0019	.0038
2.020	13.99	.3665	.3455	.7589	.7069	.0758	.0636	.3162	.011	.021	.0019	.0039
		.3295	.3356	.7336	.7101	.0681	.0324	.3219	.011	.024	.0019	.0040
		.2948	.3000	.7202	.7118	.0514	.0351	.3312	.011	.026	.0019	.0041
		.2531	.2649	.7285	.7019	.0487	.0320	.3464	.011	.028	.0019	.0042
		.3647	.3433	.6835	.6149	.1170	.0878	.4738	.004	.019	.0013	.0037
2.020	13.99	.3495	.3216	.7017	.6294	.1075	.0770	.4784	.005	.021	.0014	.0039
		.3311	.3126	.6986	.6439	.1065	.0675	.4800	.004	.023	.0013	.0040
		.2794	.2887	.6717	.6561	.0901	.0541	.4924	.004	.024	.0013	.0040
		.2509	.2513	.6546	.6941	.0862	.0512	.5090	.004	.026	.0013	.0041
		.2110	.2248	.6461	.6475	.0696	.0332	.5130	.004	.027	.0013	.0041
2.020	13.99	.1792	.1961	.6347	.6347	.0528	.0252	.5211	.004	.028	.0013	.0042
		.1681	.1817	.6397	.6462	.0406	.0201	.5218	.004	.028	.0013	.0042

CONFIDENTIAL

DECLASSIFIED

CONFIDENTIAL

17

TABLE I.- PERFORMANCE OF INLET CONFIGURATIONS - Continued  
(b) Two-shock vertical ramp inlet (hooded inlet)

$M_\infty$	$\alpha$ , deg	$\left(\frac{p_1}{p_\infty}\right)_L$	$\left(\frac{p_1}{p_\infty}\right)_R$	$\left(\frac{p_{t1}}{p_\infty}\right)_L$	$\left(\frac{p_{t1}}{p_\infty}\right)_R$	$\left(\frac{\Delta p_{t1}}{p_\infty}\right)_L$	$\left(\frac{\Delta p_{t1}}{p_\infty}\right)_R$	$C_D$	$\frac{M_7}{M_\infty}$	$\frac{H_7}{H_\infty}$	$c_{d7}$	$c_{d2}$
2.024	0	0.3573	0.3866	0.6030	0.6282	0.1015	0.1267	0.1440	---	---	---	---
		.4008	.3624	.6704	.6154	.1106	.0874	.1354	---	0.015	---	0.0033
		.3841	.3642	.6838	.6515	.0834	.0703	.1345	---	.016	---	.0034
		.3246	.3293	.6670	.6368	.0784	.0618	.1469	---	.017	---	.0035
		.3016	.3136	.6369	.6187	.0742	.0483	.1500	---	.019	---	.0036
		.2467	.2603	.6218	.6089	.0696	.0401	.1641	---	.019	---	.0038
		.2191	.2411	.6053	.5977	.0560	.0358	.1714	---	.019	---	.0037
		.1441	.1781	.6942	.6305	.1291	.0885	.1380	---	.017	---	.0035
		.3931	.3759	.7193	.6699	.0990	.0825	.1405	---	.017	---	.0035
		.3696	.3501	.7261	.6798	.0775	.0754	.1476	---	.018	---	.0036
2.026	2.00	.3016	.3130	.6741	.6453	.0702	.0540	.1611	---	.022	---	.0039
		.2479	.2735	.6456	.6256	.0610	.0510	.1775	---	.022	---	.0039
		.2271	.2572	.6338	.6174	.0534	.0427	.1841	---	.023	---	.0040
		.1972	.1933	.6322	.6157	.0441	.0388	.1998	---	.023	---	.0039
		.1442	.1399	.7713	.6995	.1310	.1033	.1902	0.013	.023	0.0019	.0039
		.3938	.3880	.7881	.7290	.0923	.0854	.1948	.013	.023	.0019	.0039
		.3418	.3253	.7902	.7409	.0586	.0699	.2105	.013	.025	.0019	.0040
		.2596	.3023	.7247	.6998	.0578	.0498	.2299	.013	.026	.0019	.0041
		.2417	.2706	.7076	.6863	.0549	.0377	.2594	.013	.026	.0019	.0042
		.1885	.2230	.6895	.6752	.0448	.0244	.2608	.013	.027	.0018	.0042
2.023	10.00	.4049	.4949	.7344	.6781	.1424	.1123	.3069	.012	.023	.0019	.0040
		.4094	.3983	.7868	.7343	.1140	.0950	.3097	.012	.024	.0019	.0040
		.3923	.3981	.8208	.7593	.0881	.0880	.3127	.012	.026	.0019	.0041
		.3413	.3691	.8342	.7823	.0508	.0688	.3244	.012	.028	.0019	.0042
		.3096	.3223	.8250	.7812	.0453	.0483	.3339	.012	.030	.0019	.0042
		.2613	.2943	.8093	.7803	.0439	.0319	.3494	.012	.031	.0019	.0042
		.2057	.2483	.7767	.7590	.0353	.0250	.3682	.012	.032	.0018	.0042
		.1999	.2008	.7600	.7458	.0341	.0187	.3833	.012	.032	.0019	.0042
		.3938	.3959	.7029	.6670	.1113	.0978	.4862	.009	.023	.0017	.0040
		.3913	.4000	.7533	.7162	.1025	.0793	.4894	.008	.023	.0017	.0040
2.028	14.00	.3805	.3828	.7868	.7442	.0830	.0730	.4892	.008	.025	.0017	.0040
		.3293	.3493	.7717	.7376	.0710	.0527	.5015	.008	.026	.0017	.0041
		.2882	.3090	.7684	.7360	.0441	.0413	.5038	.008	.026	.0018	.0041
		.2285	.2788	.7533	.7425	.0357	.0228	.5277	.006	.029	.0015	.0042
		.1765	.2662	.7441	.7401	.0221	.0175	.5382	.007	.032	.0016	.0042
		.1540	.1827	.7516	.7409	.0199	.0101	.5591	.006	.037	.0015	.0042

CONFIDENTIAL

TABLE I.- PERFORMANCE OF INLET CONFIGURATIONS - Continued  
(c) Three-shock horizontal ramp inlet

$N_{no}$	$\alpha$ , deg	$\delta$ , deg	Ramp bleed config.	$\left(\frac{m_1}{L}\right)$	$\left(\frac{m_2}{L}\right)$	$\left(\frac{P_{t1}}{P_{t2}}\right)$	$\left(\frac{P_{t1}}{P_{t2}}\right)$	$\left(\frac{P_{t1}}{P_{t2}}\right)$	$\left(\frac{\Delta P_{t1}}{P_{t2}}\right)$	$C_D$	$\frac{P_2}{P_1}$	$\frac{P_3}{P_1}$	$\frac{P_4}{P_1}$	$\frac{P_5}{P_1}$	$C_{D3}$	$C_{D4}$	$C_{D7}$	$C_{D8}$	$C_{D9}$				
2.027	2.05	12	2	.4099 .4832 .4794 .4486 .3135 .3449 .2845	.4325 .4502 .4894 .4872 .7903 .7771 .7823	.07769 .08133 .8476 .8366 .7711 .7775	.06574 .7554 .8891 .8366 .7711 .7775	.02561 .1620 .0938 .0741 .0692 .0445	.01626 .1744 .0938 .0773 .0704 .0448	—	.0003 .0004 .0003 .0005 .0005	.0028 .0221 .0222 .026 .029 .028	.0019 .017 .017 .017 .018 .016	0	0	—	.00005 .0005 .0005 .0007 .0006	.00030 .0037 .0038 .0040 .0040 .0042	.00016 .0019 .0019 .0019 .0019 .0019	0	0		
2.020	1.95	12	3	.4579 .5817 .5225 .4743 .4852 .4750 .4638 .4523 .4496 .4388 .3074 .3679	.4401 .3846 .4743 .8972 .8938 .8892 .8892 .8892 .8892 .8892 .8892 .8892	.7822 .7826 .8210 .8210 .8473 .8489 .8489 .8477 .8395 .8395 .8395 .7964	.6601 .7054 .8210 .8210 .1001 .0922 .0922 .0648 .0829 .0829 .0829 .7815	.2213 .1753 .1488 .1581 .0913 .0764 .0677 .0595 .0595 .0595 .0595 .0658	.1596 .1521 .1581 .0913 .0764 .0677 .0595 .0595 .0595 .0595 .0595 .0447	0	.022 .022 .022 .022 .026 .029 .029 .031 .031 .031 .030	.017 .017 .017 .017 .016 .016 .016 .016 .016 .016 .016	0	0	0	0	0	.0036 .0037 .0037 .0040 .0041 .0041 .0041 .0041 .0041 .0041 .0041 .0041	.00016 .0019 .0019 .0019 .0019 .0019 .0019 .0019 .0019 .0019 .0019 .0019	0	0		
2.021	2.00	12	4	.4805 .4642 .4559 .4514 .3980 .3277	.4240 .4319 .4329 .4108 .3832 .3225	.7682 .8052 .8674 .8674 .8674 .7684	.7078 .7720 .8280 .8280 .8280 .7720	.1754 .1147 .0864 .0921 .0764 .0538	.1234 .1132 .0875 .0764 .0661 .0388	0	.027 .027 .030 .040 .051 .047	.016 .016 .017 .018 .018 .017	0	0	0	0	0	.0040 .0040 .0041 .0041 .0041 .0041 .0041 .0041 .0041 .0041 .0041 .0041	.00016 .0019 .0019 .0019 .0019 .0019 .0019 .0019 .0019 .0019 .0019 .0019	0	0		
2.014	2.05	12	No bleed	.4257 .4668 .4503 .4393 .3845 .3158	.4257 .4323 .4276 .4301 .3845 .3011	.7600 .8367 .8350 .7835 .7347 .7499	.6308 .7766 .7816 .7458 .7347 .7310	.2492 .1131 .0805 .0700 .0657 .0465	.1580 .0706 .0574 .0434 .0434 .0341	0	0 .017 .017 .017 .017 .017 .016	.016 .016 .016 .016 .016 .016	0	0	0	0	0	.0017 .0017 .0021 .0025 .0024 .0024	.00016 .0019 .0019 .0019 .0019 .0019 .0019	0	0		
2.019	.05	12	1	.4659 .4617 .4041 .4007 .3291 .2900	.3934 .4044 .3902 .3902 .3291 .2900	.7376 .7766 .8174 .7892 .7892 .7279	.6548 .7193 .7691 .7596 .7596 .7160	.2199 .09640 .09169 .06333 .06333 .05624	.14710 .1242 .1441 .1473 .1473 .03835	.01435 .007 .008 .029 .023 .1917	.017 .017 .021 .029 .023 .028	.016 .017 .016 .017 .016 .015	0	0	0	0	0	.0007 .0007 .0007 .0007 .0014 .0015	.00017 .0017 .0021 .0025 .0024 .0024	.00016 .0019 .0019 .0019 .0019 .0019	0	0	
2.023	2.05	12	1	.4795 .4787 .4456 .4711 .3277 .2470	.4634 .4458 .4311 .3042 .2799	.8150 .8718 .8518 .8117 .7774	.7637 .8161 .8161 .7899 .7629	.09738 .09215 .06406 .05318 .05108	.1013 .0789 .04991 .1783 .04688	.2858 — .1539 .031 .1920	.009 — .011 .013 .013	.021 — .032 .031 .028	.016 .016 .017 .017 .016	0	0	0	0	0	.0008 — .0016 .0019 .0017	.00036 — .0042 .0041 .0041	.00016 .0019 .0019 .0019 .0019	0	0
2.020	4.00	12	1	.4609 .4477 .3833 .4587 .3570 .2393	.4393 .4182 .3870 .4173 .3890 .2901	.8489 .9040 .8923 .9040 .8560 .8409	.8116 .8541 .8410 .8541 .8218 .8103	.09938 .07135 .07063 .07135 .05734 .04132	.1009 .09762 .08200 .06275 .05734 .04286	.1671 .1707 .0840 .1698 .1939 .2128	.011 .0 .034 .036 .035 .016	.025 .034 .017 .017 .018 .017	0	0	0	0	0	.0015 .0016 .0020 .0016 .0016 .0018	.00040 .0041 .0041 .0041 .0041 .0041	.00016 .0019 .0019 .0019 .0019 .0019	0	0	
2.009	5.95	12	1	.5045 .4839 .4581 .4034 .4474 .3738 .3577 .3801 .2950 .2606	.4406 .4589 .4880 .4581 .4150 .3738 .3577 .3801 .2950 .2606	.7896 .7991 .8800 .8800 .8670 .8457 .8457 .8457 .8457 .8165	.7072 .7991 .8238 .8238 .8061 .7931 .7931 .8144 .8144 .7979	.1773 .1169 .09518 .09518 .1067 .0646 .0646 .0361 .0361 .02449	.1444 .1169 .2073 .2073 .2043 .039 .039 .039 .039 .02066	.1973 .011 .033 .010 .034 .038 .038 .019 .019 .036	.011 .032 .032 .016 .038 .038 .038 .019 .019 .018	.035 .032 .033 .016 .038 .038 .038 .019 .019 .017	.018 .016 .016 .016 .016 .016 .016 .016 .016 .016	0	0	0	0	0	.0018 .0020 .0022 .0021 .0021 .0021 .0021 .0021 .0021 .0021	.00042 .0042 .0042 .0041 .0041 .0041 .0041 .0041 .0041 .0041	.00016 .0019 .0019 .0019 .0019 .0019 .0019 .0019 .0019 .0019	0	0
2.017	9.10	12	1	.4276 .4258 .3512 .3212 .1794	.4128 .4012 .3339 .3216 .1468	.8158 .8677 .8249 .8243 .8091	.7678 .8005 .8001 .7961 .7923	.08521 .1087 .07914 .07914 .0247	.1289 .1427 .1042 .0299 .02969	.2889 .3106 .3343 .039 .0360	.013 .015 .017 .039 .020	.034 .036 .038 .039 .038	.019 .019 .019 .018	0	0	0	0	0	.0020 .0018 .0020 .0018 .0011	.00034 .0036 .0038 .0038 .0039	.00016 .0019 .0019 .0019 .0019	0	0
2.017	14.05	12	1	.4331 .4535 .4283 .3898 .3613 .2829	.3447 .3260 .3163 .3086 .3013 .2829	.6852 .7377 .7175 .7698 .7797 .7572	.6578 .6816 .6816 .7068 .7068 .7480	.09489 .05799 .05799 .05992 .04539 .03300	.5145 .5134 .4998 .4998 .4998 .5308	.011 .011 .010 .013 .013 .020	.031 .027 .027 .035 .035 .036	.015 .016 .016 .016 .016 .016	0	0	0	0	0	.0019 .0019 .0018 .0016 .0014 .0011	.00041 .0044 .0041 .0041 .0041 .0041	.00016 .0019 .0019 .0019 .0019 .0019	0	0	
2.012	0	9	1	.4717 .4600 .4242 .3552 .3029 .2733	.3940 .3972 .3843 .3731 .3309 .2893	.7508 .7923 .7810 .7361 .7361 .7210	.6482 .7053 .7533 .7227 .7091 .7077	.2109 .1445 .04765 .0498 .0761 .05180	.1368 .1022 .04765 .0498 .0761 .04152	.1422 .1427 .1457 .1536 .1540 .1735	.006 .006 .010 .013 .013 .012	.033 .034 .027 .027 .027 .024	.017 .017 .017 .017 .017 .015	0	0	0	0	0	.0003 .0005 .0008 .0008 .0012 .0014	.00029 .0029 .0029 .0029 .0029 .0029	.00016 .0019 .0019 .0019 .0019 .0019	0	0
2.017	2.00	9	1	.4859 .4788 .4400 .4021 .3913 .2996	.4149 .4450 .4240 .4042 .3913 .2996	.7982 .8418 .8271 .8103 .7814 .7563	.7044 .7619 .7967 .7934 .7854 .7520	.1878 .1343 .06867 .0498 .0498 .03709	.1502 .1453 .0591 .0591 .0591 .03709	.010 .008 .010 .011 .011 .013	.020 .015 .031 .032 .032 .017	.017 .017 .017 .017 .017 .017	0	0	0	0	0	.0012 .0008 .0014 .0014 .0014 .0017	.00037 .0033 .0042 .0042 .0042 .0041	.00016 .0019 .0019 .0019 .0019 .0019	0	0	

TABLE I.- PERFORMANCE OF INLET CONFIGURATIONS - Continued  
(c) Three-shock horizontal ramp inlet - Continued

$M_\infty$	$\alpha$ , deg	$\delta$ , deg	Ramp bleed config.	$(\frac{P_1}{P_\infty})_L$	$(\frac{P_1}{P_\infty})_R$	$(\frac{P_{t1}}{P_\infty})_L$	$(\frac{P_{t1}}{P_\infty})_R$	$(\frac{P_{t2}}{P_\infty})_L$	$(\frac{P_{t2}}{P_\infty})_R$	$(\frac{P_{t3}}{P_\infty})_L$	$(\frac{P_{t3}}{P_\infty})_R$	$C_D$	$H_B$	$H_B^*$	$H_V$	$H_B^*$	$H_V^*$	$C_{d1}$	$C_{d2}$	$C_{d3}$	$C_{d4}$	$C_{d5}$
2.017	4.05	9	1	0.5045 0.4998 0.4956 0.4928 0.4884 0.4848 0.4816 0.4789	0.4713 0.4707 0.4703 0.4701 0.4700 0.4700 0.4700 0.4700	0.8149 0.8149 0.8149 0.8149 0.8149 0.8149 0.8149 0.8149	0.7422 0.7422 0.7422 0.7422 0.7422 0.7422 0.7422 0.7422	0.1632 0.1632 0.1632 0.1632 0.1632 0.1632 0.1632 0.1632	0.1342 0.1342 0.1342 0.1342 0.1342 0.1342 0.1342 0.1342	0.1637 0.1637 0.1637 0.1637 0.1637 0.1637 0.1637 0.1637	0.010 0.009 0.009 0.009 0.009 0.009 0.009 0.009	0.021 0.021 0.021 0.021 0.021 0.021 0.021 0.021	0.017 0.017 0.017 0.017 0.017 0.017 0.017 0.017	0 0 0 0 0 0 0 0	0 0 0 0 0 0 0 0	0.0013 0.0013 0.0013 0.0013 0.0013 0.0013 0.0013 0.0013	0.0037 0.0037 0.0037 0.0037 0.0037 0.0037 0.0037 0.0037	0.0020 0.0020 0.0020 0.0020 0.0020 0.0020 0.0020 0.0020	0 0 0 0 0 0 0 0	0 0 0 0 0 0 0 0		
2.014	6.00	9	1	0.5129 0.5093 0.5058 0.5026 0.5000 0.4978 0.4956 0.4934	0.4383 0.4383 0.4383 0.4383 0.4383 0.4383 0.4383 0.4383	0.8355 0.8355 0.8355 0.8355 0.8355 0.8355 0.8355 0.8355	0.7540 0.7540 0.7540 0.7540 0.7540 0.7540 0.7540 0.7540	0.1831 0.1831 0.1831 0.1831 0.1831 0.1831 0.1831 0.1831	0.1454 0.1454 0.1454 0.1454 0.1454 0.1454 0.1454 0.1454	0.2121 0.2121 0.2121 0.2121 0.2121 0.2121 0.2121 0.2121	0.010 0.009 0.009 0.009 0.009 0.009 0.009 0.009	0.026 0.026 0.026 0.026 0.026 0.026 0.026 0.026	0.018 0.018 0.018 0.018 0.018 0.018 0.018 0.018	0 0 0 0 0 0 0 0	0 0 0 0 0 0 0 0	0.0014 0.0014 0.0014 0.0014 0.0014 0.0014 0.0014 0.0014	0.0040 0.0040 0.0040 0.0040 0.0040 0.0040 0.0040 0.0040	0.0020 0.0020 0.0020 0.0020 0.0020 0.0020 0.0020 0.0020	0 0 0 0 0 0 0 0	0 0 0 0 0 0 0 0		
2.016	10.05	9	1	0.4979 0.4906 0.4864 0.4826 0.4793 0.4761 0.4731 0.4701	0.4658 0.4658 0.4658 0.4658 0.4658 0.4658 0.4658 0.4658	0.7926 0.7926 0.7926 0.7926 0.7926 0.7926 0.7926 0.7926	0.7153 0.7153 0.7153 0.7153 0.7153 0.7153 0.7153 0.7153	0.1325 0.1325 0.1325 0.1325 0.1325 0.1325 0.1325 0.1325	0.1060 0.1060 0.1060 0.1060 0.1060 0.1060 0.1060 0.1060	0.1468 0.1468 0.1468 0.1468 0.1468 0.1468 0.1468 0.1468	0.016 0.016 0.016 0.016 0.016 0.016 0.016 0.016	0.038 0.038 0.038 0.038 0.038 0.038 0.038 0.038	0.018 0.018 0.018 0.018 0.018 0.018 0.018 0.018	0 0 0 0 0 0 0 0	0 0 0 0 0 0 0 0	0.0012 0.0012 0.0012 0.0012 0.0012 0.0012 0.0012 0.0012	0.0041 0.0041 0.0041 0.0041 0.0041 0.0041 0.0041 0.0041	0.0021 0.0021 0.0021 0.0021 0.0021 0.0021 0.0021 0.0021	0 0 0 0 0 0 0 0	0 0 0 0 0 0 0 0		
2.019	14.05	9	1	0.4299 0.4332 0.4378 0.4426 0.4478 0.4532 0.4588 0.4645	0.4303 0.4303 0.4303 0.4303 0.4303 0.4303 0.4303 0.4303	0.7117 0.7117 0.7117 0.7117 0.7117 0.7117 0.7117 0.7117	0.6656 0.6656 0.6656 0.6656 0.6656 0.6656 0.6656 0.6656	0.1450 0.1450 0.1450 0.1450 0.1450 0.1450 0.1450 0.1450	0.1198 0.1198 0.1198 0.1198 0.1198 0.1198 0.1198 0.1198	0.1937 0.1937 0.1937 0.1937 0.1937 0.1937 0.1937 0.1937	0.012 0.012 0.012 0.012 0.012 0.012 0.012 0.012	0.032 0.032 0.032 0.032 0.032 0.032 0.032 0.032	0.014 0.014 0.014 0.014 0.014 0.014 0.014 0.014	0 0 0 0 0 0 0 0	0 0 0 0 0 0 0 0	0.0017 0.0017 0.0017 0.0017 0.0017 0.0017 0.0017 0.0017	0.0041 0.0041 0.0041 0.0041 0.0041 0.0041 0.0041 0.0041	0.0020 0.0020 0.0020 0.0020 0.0020 0.0020 0.0020 0.0020	0 0 0 0 0 0 0 0	0 0 0 0 0 0 0 0		
2.018	0	6	1	0.4744 0.4657 0.4610 0.4578 0.4548 0.4520 0.4494 0.4468	0.4058 0.4058 0.4058 0.4058 0.4058 0.4058 0.4058 0.4058	0.7571 0.7571 0.7571 0.7571 0.7571 0.7571 0.7571 0.7571	0.6483 0.6483 0.6483 0.6483 0.6483 0.6483 0.6483 0.6483	0.1996 0.1996 0.1996 0.1996 0.1996 0.1996 0.1996 0.1996	0.1215 0.1215 0.1215 0.1215 0.1215 0.1215 0.1215 0.1215	0.1414 0.1414 0.1414 0.1414 0.1414 0.1414 0.1414 0.1414	0.005 0.006 0.006 0.006 0.006 0.006 0.006 0.006	0.009 0.009 0.009 0.009 0.009 0.009 0.009 0.009	0.017 0.017 0.017 0.017 0.017 0.017 0.017 0.017	0 0 0 0 0 0 0 0	0 0 0 0 0 0 0 0	0.0004 0.0005 0.0005 0.0005 0.0005 0.0005 0.0005 0.0005	0.0022 0.0022 0.0022 0.0022 0.0022 0.0022 0.0022 0.0022	0.0020 0.0020 0.0020 0.0020 0.0020 0.0020 0.0020 0.0020	0 0 0 0 0 0 0 0	0 0 0 0 0 0 0 0		
2.018	1.95	6	1	0.4962 0.4924 0.4894 0.4864 0.4834 0.4804 0.4774 0.4744	0.4479 0.4479 0.4479 0.4479 0.4479 0.4479 0.4479 0.4479	0.7909 0.7909 0.7909 0.7909 0.7909 0.7909 0.7909 0.7909	0.6927 0.6927 0.6927 0.6927 0.6927 0.6927 0.6927 0.6927	0.1748 0.1748 0.1748 0.1748 0.1748 0.1748 0.1748 0.1748	0.1123 0.1123 0.1123 0.1123 0.1123 0.1123 0.1123 0.1123	0.1458 0.1458 0.1458 0.1458 0.1458 0.1458 0.1458 0.1458	0.008 0.008 0.008 0.008 0.008 0.008 0.008 0.008	0.015 0.015 0.015 0.015 0.015 0.015 0.015 0.015	0.016 0.016 0.016 0.016 0.016 0.016 0.016 0.016	0 0 0 0 0 0 0 0	0 0 0 0 0 0 0 0	0.0010 0.0010 0.0010 0.0010 0.0010 0.0010 0.0010 0.0010	0.0032 0.0032 0.0032 0.0032 0.0032 0.0032 0.0032 0.0032	0.0021 0.0021 0.0021 0.0021 0.0021 0.0021 0.0021 0.0021	0 0 0 0 0 0 0 0	0 0 0 0 0 0 0 0		
2.018	4.05	6	1	0.5066 0.5044 0.5022 0.5000 0.4978 0.4956 0.4934 0.4912	0.4732 0.4732 0.4732 0.4732 0.4732 0.4732 0.4732 0.4732	0.8138 0.8138 0.8138 0.8138 0.8138 0.8138 0.8138 0.8138	0.7348 0.7348 0.7348 0.7348 0.7348 0.7348 0.7348 0.7348	0.1491 0.1491 0.1491 0.1491 0.1491 0.1491 0.1491 0.1491	0.1247 0.1247 0.1247 0.1247 0.1247 0.1247 0.1247 0.1247	0.1652 0.1652 0.1652 0.1652 0.1652 0.1652 0.1652 0.1652	0.009 0.009 0.009 0.009 0.009 0.009 0.009 0.009	0.020 0.020 0.020 0.020 0.020 0.020 0.020 0.020	0.017 0.017 0.017 0.017 0.017 0.017 0.017 0.017	0 0 0 0 0 0 0 0	0 0 0 0 0 0 0 0	0.0011 0.0011 0.0011 0.0011 0.0011 0.0011 0.0011 0.0011	0.0035 0.0035 0.0035 0.0035 0.0035 0.0035 0.0035 0.0035	0.0020 0.0020 0.0020 0.0020 0.0020 0.0020 0.0020 0.0020	0 0 0 0 0 0 0 0	0 0 0 0 0 0 0 0		
2.015	6.05	6	1	0.5289 0.5255 0.5222 0.5188 0.5154 0.5120 0.5086 0.5052	0.4889 0.4889 0.4889 0.4889 0.4889 0.4889 0.4889 0.4889	0.8242 0.8242 0.8242 0.8242 0.8242 0.8242 0.8242 0.8242	0.7352 0.7352 0.7352 0.7352 0.7352 0.7352 0.7352 0.7352	0.1864 0.1864 0.1864 0.1864 0.1864 0.1864 0.1864 0.1864	0.1388 0.1388 0.1388 0.1388 0.1388 0.1388 0.1388 0.1388	0.1964 0.1964 0.1964 0.1964 0.1964 0.1964 0.1964 0.1964	0.009 0.009 0.009 0.009 0.009 0.009 0.009 0.009	0.025 0.025 0.025 0.025 0.025 0.025 0.025 0.025	0.018 0.018 0.018 0.018 0.018 0.018 0.018 0.018	0 0 0 0 0 0 0 0	0 0 0 0 0 0 0 0	0.0015 0.0015 0.0015 0.0015 0.0015 0.0015 0.0015 0.0015	0.0039 0.0039 0.0039 0.0039 0.0039 0.0039 0.0039 0.0039	0.0021 0.0021 0.0021 0.0021 0.0021 0.0021 0.0021 0.0021	0 0 0 0 0 0 0 0	0 0 0 0 0 0 0 0		
2.012	10.05	6	1	0.5293 0.5266 0.5238 0.5210 0.5182 0.5154 0.5126 0.5098	0.4899 0.4899 0.4899 0.4899 0.4899 0.4899 0.4899 0.4899	0.8126 0.8126 0.8126 0.8126 0.8126 0.8126 0.8126 0.8126	0.7385 0.7385 0.7385 0.7385 0.7385 0.7385 0.7385 0.7385	0.1780 0.1780 0.1780 0.1780 0.1780 0.1780 0.1780 0.1780	0.1322 0.1322 0.1322 0.1322 0.1322 0.1322 0.1322 0.1322	0.2784 0.2784 0.2784 0.2784 0.2784 0.2784 0.2784 0.2784	0.010 0.010 0.010 0.010 0.010 0.010 0.010 0.010	0.036 0.036 0.036 0.036 0.036 0.036 0.036 0.036	0.019 0.019 0.019 0.019 0.019 0.019 0.019 0.019	0 0 0 0 0 0 0 0	0 0 0 0 0 0 0 0	0.0019 0.0019 0.0019 0.0019 0.0019 0.0019 0.0019 0.0019	0.0041 0.0041 0.0041 0.0041 0.0041 0.0041 0.0041 0.0041	0.0021 0.0021 0.0021 0.0021 0.0021 0.0021 0.0021 0.0021	0 0 0 0 0 0 0 0	0 0 0 0 0 0 0 0		
2.015	14.00	6	1	0.4603 0.4583 0.4563 0.4543 0.4523 0.4503 0.4483 0.4463	0.4472 0.4472 0.4472 0.4472 0.4472 0.4472 0.4472 0.4472	0.7058 0.7058 0.7058 0.7058 0.7058 0.7058 0.7058 0.7058	0.6210 0.6210 0.6210 0.6210 0.6210 0.6210 0.6210 0.6210	0.1210 0.1210 0.1210 0.1210 0.1210 0.1210 0.1210 0.1210	0.1011 0.1011 0.1011 0.1011 0.1011 0.1011 0.1011 0.1011	0.1438 0.1438 0.1438 0.1438 0.1438 0.1438 0.1438 0.1438	0.012 0.012 0.012 0.012 0.012 0.012 0.012 0.012	0.035 0.035 0.035 0.035 0.035 0.035 0.035 0.035	0.014 0.014 0.014 0.014 0.014 0.014 0.014 0.014	0 0 0 0 0 0 0 0	0 0 0 0 0 0 0 0	0.0015 0.0015 0.0015 0.0015 0.0015 0.0015 0.0015 0.0015	0.0041 0.0041 0.0041 0.0041 0.0041 0.0041 0.0041 0.0041	0.0022 0.0022 0.0022 0.0022 0.0022 0.0022 0.0022 0.0022	0 0 0 0 0 0 0 0	0 0 0 0 0 0 0 0		
2.014	0	0	1	0.4626 0.4607 0.4587 0.4567 0.4547 0.4527 0.4507 0.4487	0.4193 0.4193 0.4193 0.4193 0.4193 0.4193 0.4193 0.4193	0.7398 0.7398 0.7398 0.7398 0.7398 0.7398 0.7398 0.7398	0.6766 0.6766 0.6766 0.6766 0.6766 0.6766 0.6766 0.6766	0.1319 0.1319 0.1319 0.1319 0.1319 0.1319 0.1319 0.1319	0.1036 0.1036 0.1036 0.1036 0.1036 0.1036 0.1036 0.1036	0.1405 0.1405 0.1405 0.1405 0.1405 0.1405 0.1405 0.1405	0.003 0.004 0.004 0.004 0.004 0.004 0.004 0.004	0.012 0.012 0.012 0.012 0.012 0.012 0.012 0.012	0.014 0.014 0.014 0.014 0.014 0.014 0.014 0.014	0 0 0 0 0 0 0 0	0 0 0 0 0 0 0 0	0.0005 0.0004 0.0004 0.0004 0.0004 0.0004 0.0004 0.0004	0.0027 0.0023 0.0024 0.0024 0.0024 0.0024 0.0024 0.0024	0.0021 0.0020 0.0020 0.0020 0.0020 0.0020 0.0020 0.0020	0 0 0 0 0 0 0 0	0 0 0 0 0 0 0 0		

CONFIDENTIAL

$\lambda_{\text{vac}}$	$\alpha$ , deg	$\delta$ , deg	Ramp bleed config.	$\left(\frac{P_{11}}{P_{10}}\right)_L$	$\left(\frac{P_{11}}{P_{10}}\right)_R$	$\left(\frac{P_{21}}{P_{20}}\right)_L$	$\left(\frac{P_{21}}{P_{20}}\right)_R$	$\left(\frac{P_{31}}{P_{30}}\right)_L$	$\left(\frac{P_{31}}{P_{30}}\right)_R$	$C_D$	$\frac{M_0}{M_1}$	$\frac{M_0}{M_2}$	$\frac{M_0}{M_3}$	$\frac{M_0}{M_4}$	$\frac{M_0}{M_5}$	$\frac{M_0}{M_6}$	$\frac{M_0}{M_7}$	$\frac{M_0}{M_8}$	$\frac{M_0}{M_9}$	$\frac{M_0}{M_{10}}$	$\frac{M_0}{M_{11}}$	$\frac{M_0}{M_{12}}$	$\frac{M_0}{M_{13}}$	$\frac{M_0}{M_{14}}$	$\frac{M_0}{M_{15}}$	$\frac{M_0}{M_{16}}$	$\frac{M_0}{M_{17}}$	$\frac{M_0}{M_{18}}$	$\frac{M_0}{M_{19}}$	$\frac{M_0}{M_{20}}$	$\frac{M_0}{M_{21}}$	$\frac{M_0}{M_{22}}$	$\frac{M_0}{M_{23}}$	$\frac{M_0}{M_{24}}$	$\frac{M_0}{M_{25}}$	$\frac{M_0}{M_{26}}$	$\frac{M_0}{M_{27}}$	$\frac{M_0}{M_{28}}$	$\frac{M_0}{M_{29}}$	$\frac{M_0}{M_{30}}$	$\frac{M_0}{M_{31}}$	$\frac{M_0}{M_{32}}$	$\frac{M_0}{M_{33}}$	$\frac{M_0}{M_{34}}$	$\frac{M_0}{M_{35}}$	$\frac{M_0}{M_{36}}$	$\frac{M_0}{M_{37}}$	$\frac{M_0}{M_{38}}$	$\frac{M_0}{M_{39}}$	$\frac{M_0}{M_{40}}$	$\frac{M_0}{M_{41}}$	$\frac{M_0}{M_{42}}$	$\frac{M_0}{M_{43}}$	$\frac{M_0}{M_{44}}$	$\frac{M_0}{M_{45}}$	$\frac{M_0}{M_{46}}$	$\frac{M_0}{M_{47}}$	$\frac{M_0}{M_{48}}$	$\frac{M_0}{M_{49}}$	$\frac{M_0}{M_{50}}$	$\frac{M_0}{M_{51}}$	$\frac{M_0}{M_{52}}$	$\frac{M_0}{M_{53}}$	$\frac{M_0}{M_{54}}$	$\frac{M_0}{M_{55}}$	$\frac{M_0}{M_{56}}$	$\frac{M_0}{M_{57}}$	$\frac{M_0}{M_{58}}$	$\frac{M_0}{M_{59}}$	$\frac{M_0}{M_{60}}$	$\frac{M_0}{M_{61}}$	$\frac{M_0}{M_{62}}$	$\frac{M_0}{M_{63}}$	$\frac{M_0}{M_{64}}$	$\frac{M_0}{M_{65}}$	$\frac{M_0}{M_{66}}$	$\frac{M_0}{M_{67}}$	$\frac{M_0}{M_{68}}$	$\frac{M_0}{M_{69}}$	$\frac{M_0}{M_{70}}$	$\frac{M_0}{M_{71}}$	$\frac{M_0}{M_{72}}$	$\frac{M_0}{M_{73}}$	$\frac{M_0}{M_{74}}$	$\frac{M_0}{M_{75}}$	$\frac{M_0}{M_{76}}$	$\frac{M_0}{M_{77}}$	$\frac{M_0}{M_{78}}$	$\frac{M_0}{M_{79}}$	$\frac{M_0}{M_{80}}$	$\frac{M_0}{M_{81}}$	$\frac{M_0}{M_{82}}$	$\frac{M_0}{M_{83}}$	$\frac{M_0}{M_{84}}$	$\frac{M_0}{M_{85}}$	$\frac{M_0}{M_{86}}$	$\frac{M_0}{M_{87}}$	$\frac{M_0}{M_{88}}$	$\frac{M_0}{M_{89}}$	$\frac{M_0}{M_{90}}$	$\frac{M_0}{M_{91}}$	$\frac{M_0}{M_{92}}$	$\frac{M_0}{M_{93}}$	$\frac{M_0}{M_{94}}$	$\frac{M_0}{M_{95}}$	$\frac{M_0}{M_{96}}$	$\frac{M_0}{M_{97}}$	$\frac{M_0}{M_{98}}$	$\frac{M_0}{M_{99}}$	$\frac{M_0}{M_{100}}$	$\frac{M_0}{M_{101}}$	$\frac{M_0}{M_{102}}$	$\frac{M_0}{M_{103}}$	$\frac{M_0}{M_{104}}$	$\frac{M_0}{M_{105}}$	$\frac{M_0}{M_{106}}$	$\frac{M_0}{M_{107}}$	$\frac{M_0}{M_{108}}$	$\frac{M_0}{M_{109}}$	$\frac{M_0}{M_{110}}$	$\frac{M_0}{M_{111}}$	$\frac{M_0}{M_{112}}$	$\frac{M_0}{M_{113}}$	$\frac{M_0}{M_{114}}$	$\frac{M_0}{M_{115}}$	$\frac{M_0}{M_{116}}$	$\frac{M_0}{M_{117}}$	$\frac{M_0}{M_{118}}$	$\frac{M_0}{M_{119}}$	$\frac{M_0}{M_{120}}$	$\frac{M_0}{M_{121}}$	$\frac{M_0}{M_{122}}$	$\frac{M_0}{M_{123}}$	$\frac{M_0}{M_{124}}$	$\frac{M_0}{M_{125}}$	$\frac{M_0}{M_{126}}$	$\frac{M_0}{M_{127}}$	$\frac{M_0}{M_{128}}$	$\frac{M_0}{M_{129}}$	$\frac{M_0}{M_{130}}$	$\frac{M_0}{M_{131}}$	$\frac{M_0}{M_{132}}$	$\frac{M_0}{M_{133}}$	$\frac{M_0}{M_{134}}$	$\frac{M_0}{M_{135}}$	$\frac{M_0}{M_{136}}$	$\frac{M_0}{M_{137}}$	$\frac{M_0}{M_{138}}$	$\frac{M_0}{M_{139}}$	$\frac{M_0}{M_{140}}$	$\frac{M_0}{M_{141}}$	$\frac{M_0}{M_{142}}$	$\frac{M_0}{M_{143}}$	$\frac{M_0}{M_{144}}$	$\frac{M_0}{M_{145}}$	$\frac{M_0}{M_{146}}$	$\frac{M_0}{M_{147}}$	$\frac{M_0}{M_{148}}$	$\frac{M_0}{M_{149}}$	$\frac{M_0}{M_{150}}$	$\frac{M_0}{M_{151}}$	$\frac{M_0}{M_{152}}$	$\frac{M_0}{M_{153}}$	$\frac{M_0}{M_{154}}$	$\frac{M_0}{M_{155}}$	$\frac{M_0}{M_{156}}$	$\frac{M_0}{M_{157}}$	$\frac{M_0}{M_{158}}$	$\frac{M_0}{M_{159}}$	$\frac{M_0}{M_{160}}$	$\frac{M_0}{M_{161}}$	$\frac{M_0}{M_{162}}$	$\frac{M_0}{M_{163}}$	$\frac{M_0}{M_{164}}$	$\frac{M_0}{M_{165}}$	$\frac{M_0}{M_{166}}$	$\frac{M_0}{M_{167}}$	$\frac{M_0}{M_{168}}$	$\frac{M_0}{M_{169}}$	$\frac{M_0}{M_{170}}$	$\frac{M_0}{M_{171}}$	$\frac{M_0}{M_{172}}$	$\frac{M_0}{M_{173}}$	$\frac{M_0}{M_{174}}$	$\frac{M_0}{M_{175}}$	$\frac{M_0}{M_{176}}$	$\frac{M_0}{M_{177}}$	$\frac{M_0}{M_{178}}$	$\frac{M_0}{M_{179}}$	$\frac{M_0}{M_{180}}$	$\frac{M_0}{M_{181}}$	$\frac{M_0}{M_{182}}$	$\frac{M_0}{M_{183}}$	$\frac{M_0}{M_{184}}$	$\frac{M_0}{M_{185}}$	$\frac{M_0}{M_{186}}$	$\frac{M_0}{M_{187}}$	$\frac{M_0}{M_{188}}$	$\frac{M_0}{M_{189}}$	$\frac{M_0}{M_{190}}$	$\frac{M_0}{M_{191}}$	$\frac{M_0}{M_{192}}$	$\frac{M_0}{M_{193}}$	$\frac{M_0}{M_{194}}$	$\frac{M_0}{M_{195}}$	$\frac{M_0}{M_{196}}$	$\frac{M_0}{M_{197}}$	$\frac{M_0}{M_{198}}</$
------------------------	-------------------	-------------------	--------------------------	--	--	--	--	--	--	-------	-------------------	-------------------	-------------------	-------------------	-------------------	-------------------	-------------------	-------------------	-------------------	----------------------	----------------------	----------------------	----------------------	----------------------	----------------------	----------------------	----------------------	----------------------	----------------------	----------------------	----------------------	----------------------	----------------------	----------------------	----------------------	----------------------	----------------------	----------------------	----------------------	----------------------	----------------------	----------------------	----------------------	----------------------	----------------------	----------------------	----------------------	----------------------	----------------------	----------------------	----------------------	----------------------	----------------------	----------------------	----------------------	----------------------	----------------------	----------------------	----------------------	----------------------	----------------------	----------------------	----------------------	----------------------	----------------------	----------------------	----------------------	----------------------	----------------------	----------------------	----------------------	----------------------	----------------------	----------------------	----------------------	----------------------	----------------------	----------------------	----------------------	----------------------	----------------------	----------------------	----------------------	----------------------	----------------------	----------------------	----------------------	----------------------	----------------------	----------------------	----------------------	----------------------	----------------------	----------------------	----------------------	----------------------	----------------------	----------------------	----------------------	----------------------	----------------------	----------------------	----------------------	----------------------	----------------------	----------------------	----------------------	----------------------	----------------------	-----------------------	-----------------------	-----------------------	-----------------------	-----------------------	-----------------------	-----------------------	-----------------------	-----------------------	-----------------------	-----------------------	-----------------------	-----------------------	-----------------------	-----------------------	-----------------------	-----------------------	-----------------------	-----------------------	-----------------------	-----------------------	-----------------------	-----------------------	-----------------------	-----------------------	-----------------------	-----------------------	-----------------------	-----------------------	-----------------------	-----------------------	-----------------------	-----------------------	-----------------------	-----------------------	-----------------------	-----------------------	-----------------------	-----------------------	-----------------------	-----------------------	-----------------------	-----------------------	-----------------------	-----------------------	-----------------------	-----------------------	-----------------------	-----------------------	-----------------------	-----------------------	-----------------------	-----------------------	-----------------------	-----------------------	-----------------------	-----------------------	-----------------------	-----------------------	-----------------------	-----------------------	-----------------------	-----------------------	-----------------------	-----------------------	-----------------------	-----------------------	-----------------------	-----------------------	-----------------------	-----------------------	-----------------------	-----------------------	-----------------------	-----------------------	-----------------------	-----------------------	-----------------------	-----------------------	-----------------------	-----------------------	-----------------------	-----------------------	-----------------------	-----------------------	-----------------------	-----------------------	-----------------------	-----------------------	-----------------------	-----------------------	-----------------------	-----------------------	-----------------------	-----------------------	-----------------------	-----------------------	-----------------------	-------------------------

[illegible]

CONFIDENTIAL

TABLE I.- PERFORMANCE OF INLET CONFIGURATIONS - Continued  
(d) Internal compression inlet

$K_L$	$\alpha$ , deg	Flow deflector plate config.	Centerbody bleed config.	$(\frac{P_{t1}}{P_{t0}})_L$	$(\frac{P_{t1}}{P_{t0}})_R$	$(\frac{P_{t1}}{P_{t0}})_L$	$(\frac{P_{t1}}{P_{t0}})_R$	$(\frac{P_{t1}}{P_{t0}})_L$	$(\frac{P_{t1}}{P_{t0}})_R$	$C_D$	$\frac{P_{t1}}{P_{t0}}$	$\frac{P_{t1}}{P_{t0}}$	$\frac{P_{t1}}{P_{t0}}$	$C_{D0}$	$C_{D0}$	$C_{D1}$	$\frac{A_{min}}{A_1}$
2.025	1.98	---	1	---	---	0.8619	0.8588	0.1042	0.0784	---	0.010	0.029	0.014	0.0028	0.0017	0.0019	0.6958
2.024	2.00	---	1	---	---	.8636	.8654	.1034	.0807	---	.010	.027	.014	.0028	.0022	.0019	.6975
2.027	2.00	---	1	---	---	.8787	.8753	.0994	.0768	---	.012	.028	.014	.0030	.0021	.0019	.6992
2.021	2.00	---	1	---	---	.8724	.8708	.1001	.0774	---	.010	.028	.014	.0027	.0021	.0019	.7005
2.018	2.00	---	1	---	---	.8674	.8658	.1007	.0750	---	.020	.033	.014	.0038	.0018	.0019	.7060
2.025	1.98	---	1	---	---	.8691	.8708	.1036	.0804	---	.010	.028	---	.0027	.0022	---	.6995
2.025	1.98	---	1	---	---	.8607	.8609	.1075	.0814	---	.010	.024	---	.0026	.0019	---	.6958
2.025	1.98	---	1	---	---	.8691	.8725	.1007	.0774	---	.010	.028	---	.0025	.0023	---	.7035
2.025	1.98	---	1	---	---	.8662	.8680	.0867	---	---	.016	.028	---	.0039	.0022	---	.7085
2.008	2.00	---	3	---	---	.8727	.8725	.0625	.0609	---	.013	.029	.014	.0031	.0027	.0020	.694
2.011	2.00	---	3	---	---	.8781	.8763	.0566	.0569	---	.026	.031	.013	.0042	.0029	---	.699
2.011	2.05	---	3	---	---	.8827	.8725	.0506	.0482	---	.014	.032	.013	.0033	.0029	---	.7045
2.011	2.05	---	3	---	---	.8626	.8513	.0547	.0512	---	.014	.030	.014	.0033	.0028	---	.7102
2.011	2.05	---	3	---	---	.8526	.8365	.0524	.0525	---	.011	.032	.014	.0027	.0028	---	.7218
2.008	2.05	---	3	---	---	.8459	.8251	.0411	.0534	---	.021	.026	.014	.0029	.0023	---	.734
2.018	2.00	---	3	---	---	.8782	.8698	.0708	.0715	---	.013	.028	.014	.0031	.0027	---	.6938
2.015	2.05	---	3	---	---	.8799	.8698	---	---	---	.011	.031	.014	.0029	.0030	---	.699
2.014	2.00	---	3	---	---	.8480	.8534	.0558	.0525	---	.011	.029	.013	.0030	.0028	---	.7102
2.009	1.95	---	2	---	---	.8718	.8700	.0797	.0656	---	.016	.028	.013	.0031	.0024	.0020	.6862
2.009	1.95	---	2	---	---	.8768	.8733	.0764	.0653	---	.011	.031	.014	.0027	.0026	---	.6875
2.003	1.95	---	2	---	---	.8752	.8733	.0765	.0596	---	.017	.028	.013	.0033	.0023	---	.690
2.009	1.95	---	2	---	---	.8718	.8749	.0711	.0539	---	.010	.033	.014	.0026	.0027	---	.698
2.006	1.95	---	2	---	---	.8489	.8607	.0565	.0721	---	.011	.027	.014	.0027	.0024	---	.7042
2.055	0	None	No bleed	---	---	.8110	.7551	.0828	.0993	---	0	0	---	0	0	0	.712
2.029	-0.05	---	No bleed	---	---	.8330	.7762	.0717	.1084	---	0	0	---	0	0	0	.712
2.029	-0.05	---	No bleed	---	---	.8296	.7746	.0726	.1093	---	0	0	---	0	0	0	.7108
2.027	-0.05	---	No bleed	---	---	.8197	.8065	.0826	.1113	---	0	0	---	0	0	0	.7097
2.025	-15	---	No bleed	---	---	.8173	.7706	.0765	.1149	---	0	0	---	0	0	0	.7073
2.020	1.73	---	No bleed	---	---	.8164	.8167	.0785	.0821	---	0	0	---	0	0	0	.6930
2.032	1.93	---	No bleed	---	---	.8141	.8096	.0844	.0966	---	0	0	---	0	0	0	.7090
2.026	1.98	---	No bleed	---	---	.8083	.8043	.0852	.0950	---	0	0	---	0	0	0	.7093
2.025	1.88	---	No bleed	---	---	.8198	.8044	.0838	.0992	---	0	0	---	0	0	0	.7024
2.022	1.88	---	No bleed	---	---	.8159	.8084	.0815	.0933	---	0	0	---	0	0	0	.6992
2.028	3.91	---	No bleed	---	---	.8380	.8106	.0568	.0920	---	0	0	---	0	0	0	.7090
2.025	3.91	---	No bleed	---	---	.840	.813	.0596	.1004	---	0	0	---	0	0	0	.7024
2.026	3.96	---	No bleed	---	---	.8284	.8225	.0797	.0623	---	0	0	---	0	0	0	.6992
2.020	5.99	---	No bleed	---	---	.8069	.8044	.0799	.0958	---	0	0	---	0	0	0	.7229
2.017	5.84	---	No bleed	---	---	.8134	.8134	.0770	.0945	---	0	0	---	0	0	0	.7229
2.026	5.94	---	No bleed	---	---	.8152	.8132	.0781	.0991	---	0	0	---	0	0	0	.720
2.026	7.97	---	No bleed	---	---	.8042	.8040	.0827	.1209	---	0	0	---	0	0	0	.7325
2.023	7.97	---	No bleed	---	---	.8110	.8151	.0752	.1252	---	0	0	---	0	0	0	.7313
2.023	7.92	---	No bleed	---	---	.8090	.8023	.0760	.1219	---	0	0	---	0	0	0	.7320
2.023	9.55	---	No bleed	---	---	.8033	.8003	.0704	.1173	---	0	0	---	0	0	0	.7400
2.026	9.80	---	No bleed	---	---	.8057	.8035	.0638	.1055	---	0	0	---	0	0	0	.7400
2.010	-0.05	---	No bleed	---	---	.8063	.8010	.0803	.0909	---	0.1250	.011	.023	.014	.0024	.0028	.7017
2.026	-0.05	---	No bleed	---	---	.8033	.8003	.0704	.1173	---	0.1250	.011	.023	.014	.0024	.0028	.7017
2.004	0	---	No bleed	---	---	.8078	.8027	.0810	.0927	---	0.1250	.012	.025	.014	.0025	.0027	.7102
2.010	0	---	No bleed	---	---	.8050	.8033	.0803	.0909	---	0.1250	.012	.025	.014	.0025	.0027	.7220
2.011	2.00	---	No bleed	---	---	.8078	.8027	.0810	.0927	---	0.1250	.013	.030	.014	.0027	.0031	.6940
2.011	2.05	---	No bleed	---	---	.8078	.8033	.0803	.0909	---	0.1250	.026	.031	.013	.0029	.0042	.6990
2.011	2.05	---	No bleed	---	---	.8005	.8015	.0827	.0925	---	0.1250	.014	.032	.013	.0029	.0033	.7045
2.011	2.00	---	No bleed	---	---	.8025	.8013	.0818	.0918	---	0.1250	---	---	.0028	.0033	.0020	.7102
2.004	4.05	None	3	---	---	.8227	.8036	.0845	.0497	---	.011	.029	.014	.0027	.0028	.0021	.6980
2.006	3.95	---	3	---	---	.8221	.8036	.0845	.0490	---	.011	.033	.014	.0029	.0028	.0020	.7040
2.007	4.00	---	3	---	---	.8255	.8043	.0832	.0437	---	.011	.033	.014	.0028	.0028	.0020	.7102
2.004	3.95	---	3	---	---	.8277	.8040	.0822	.0464	---	.011	.033	.015	.0028	.0028	.0020	.7215
2.007	6.00	---	3	---	---	.8203	.8045	.0815	.0464	---	.011	.033	.015	.0028	.0028	.0020	.7117
2.004	6.00	---	3	---	---	.8221	.8040	.0822	.0464	---	.011	.033	.015	.0028	.0028	.0020	.7215
2.010	5.95	---	3	---	---	.8221	.8040	.0822	.0464	---	.011	.033	.015	.0028	.0028	.0020	.7167
2.007	6.00	---	3	---	---	.8221	.8040	.0822	.0464	---	.011	.033	.015	.0028	.0028	.0020	.7310
2.007	5.95	---	3	---	---	.8221	.8040	.0822	.0464	---	.011	.033	.015	.0028	.0028	.0020	.7338
2.007	10.05	---	3	---	---	.8221	.8040	.0822	.0464	---	.011	.033	.015	.0028	.0028	.0020	.7333
2.007	10.00	---	3	---	---	.8221	.8040	.0822	.0464	---	.011	.033	.015	.0028	.0028	.0020	.7340
2.004	10.00	---	3	---	---	.8221	.8040	.0822	.0464	---	.011	.033	.015	.0028	.0028	.0020	.7340
2.007	14.05	---	3	---	---	.8221	.8040	.0822	.0464	---	.011	.033	.015	.0028	.0028	.0020	.7340
2.006	14.10	---	3	---	---	.8221	.8040	.0822	.0464	---	.011	.033	.015	.0028	.0028	.0020	.7340
2.012	0	---	1	---	---	.8221	.8040	.0822	.0464	---	.011	.033	.015	.0028	.0028	.0020	.6965
2.006	0	---	1	---	---	.8221	.8040	.0822	.0464	---	.011	.033	.015	.0028	.0028	.0020	.6980
2.011	0	---	1	---	---	.8221	.8040	.0822	.0464	---	.011	.033	.015	.0028	.0028	.0020	.7005
2.012	0	---	1	---	---	.8221	.8040	.0822	.0464	---	.011	.033	.015	.0028	.0028	.0020	.7053
2.009	2.05	---	1	---	---	.8221	.8040	.0822	.0464	---	.011	.033	.015	.0028	.0028	.0020	.7161
2.012	2.05	---	1	---	---	.8221	.8040	.0822	.0464	---	.011	.033	.015	.0028	.0028	.0020	.7040
2.006	2.05	---	1	---	---	.8221	.8040	.0822	.0464	---	.011	.033	.015	.0028	.0028	.0020	.7080
2.006	2.05	---	1	---	---	.8221	.8040	.0822	.0464	---	.011	.033	.015	.0028	.0028	.0020	.7150
2.009	4.00	---	1	---	---	.8221	.8040	.0822	.0464	---	.011	.033	.015	.0028	.0028	.0020	.7338
2.006	4.00	---	1	---	---	.8221	.8040	.0822	.0464	---	.011	.033	.015	.0028	.0028	.0020	.7161
2.006	4.00	---	1	---	---	.8221	.8040	.0822	.0464	---	.011	.033	.015	.0028	.0028	.0020	.7215
2.009	4.00	---	1	---	---	.8221	.8040	.0822	.0464	---	.011	.033	.015	.0028	.0028	.0020	.7264
2.011	4.00	---	1	---	---	.8221	.8040	.0822	.0464	---	.011	.033	.015	.0028	.0028	.0020	.7330
2.008	4.00	---	1	---	---	.8221	.8040	.0822	.0464	---	.011	.033	.015	.0028	.0028	.0020	.7275
2.011	5.95	---	1	---	---	.8221	.8040	.0822	.0464	---	.011	.033	.015	.0028	.0028	.0020	.7310
2.008	6.00	---	1	---	---	.8221	.8040	.0822	.0464	---	.011	.033	.015	.0028	.0028	.0020	.7257

CONFIDENTIAL

TABLE I.- PERFORMANCE OF INLET CONFIGURATIONS - Concluded  
(d) Internal compression inlet - Concluded

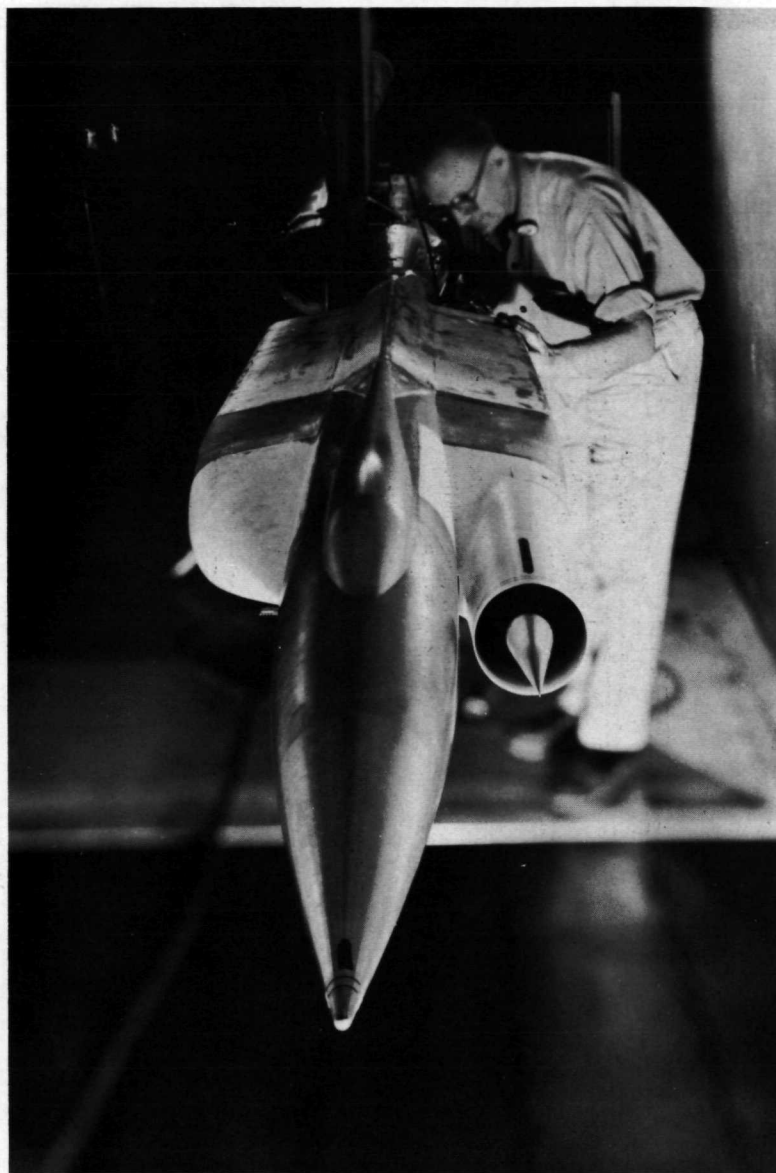
$M_0$	$\alpha$ , deg	Flow deflector plate config.	Centerbody bleed config.	$(\frac{P}{P_0})_L$	$(\frac{P}{P_0})_R$	$(\frac{P}{P_0})_{L,R}$	$(\frac{P}{P_0})_{L,R}$	$(\frac{P}{P_0})_{L,R}$	$(\frac{P}{P_0})_{L,R}$	$C_D$	$\frac{M}{M_0}$	$\frac{P}{P_0}$	$\frac{P}{P_0}$	$\frac{P}{P_0}$	$C_{D0}$	$C_{D0}$	$C_{D0}$	$\frac{A_{min}}{A_1}$
2.008	6.00	1	3	0.4916	0.4951	0.8861	0.8562	0.0644	0.0638	0.1844	0.012	0.035	0.015	0.0029	0.0029	0.0029	0.7338	
2.012	10.00			---	---	---	---	---	---	---	---	---	---	---	---	---	---	
2.011	10.00			0.5114	0.8876	0.8478	0.0846	0.0915	0.2898	0.012	0.026	0.016	0.0029	0.0029	0.0029	0.7340		
2.012	10.00			0.5146	0.8872	0.8473	0.0789	0.0879	0.2847	0.010	0.026	0.016	0.0027	0.0029	0.0021	0.734		
2.012	10.00			0.5166	0.8855	0.8457	0.0678	0.0897	0.2895	0.011	0.026	0.016	0.0028	0.0032	0.0021	0.734		
2.014	10.00			0.5145	0.8899	0.8771	0.8391	0.0656	0.0864	0.2895	0.011	0.027	0.016	0.0028	0.0031	0.0021	0.734	
2.014	10.00			0.5145	0.8899	0.8771	0.8391	0.0656	0.0864	0.2895	0.011	0.027	0.016	0.0028	0.0031	0.0021	0.734	
2.004	14.05			0.4884	0.4961	0.8454	0.8133	0.0888	0.0974	0.4672	0.013	0.030	0.015	0.0031	0.0036	0.0022	0.734	
2.006	0			---	---	---	---	---	---	---	---	---	---	---	---	---	---	
2.006	0			0.4859	0.4740	0.8395	0.8214	0.0716	0.0958	0.1319	0.012	0.024	0.014	0.0027	0.0023	0.0020	0.7102	
2.003	0			0.4781	0.4645	0.8300	0.8193	0.0720	0.0456	0.1332	0.012	0.024	0.014	0.0028	0.0025	0.0020	0.7163	
2.005	0			0.4860	0.4639	0.8325	0.8152	0.0539	0.0428	0.1317	0.012	0.023	0.014	0.0027	0.0025	0.0020	0.7215	
2.005	2.05			---	---	---	---	---	---	---	---	---	---	---	---	---	---	
2.006	2.05			0.4836	0.4685	0.8774	0.8674	0.0619	0.0546	0.1334	0.014	0.032	0.014	0.0032	0.0029	0.0020	0.7045	
2.005	2.05			0.4841	0.4995	0.8678	0.8481	0.0517	0.0476	0.1334	0.014	0.031	0.014	0.0030	0.0029	0.0020	0.7161	
2.009	4.05			0.4971	0.4818	0.8652	0.8553	0.0489	0.0437	0.1466	0.013	0.029	0.014	0.0030	0.0029	0.0020	0.6960	
2.008	4.05			0.4886	0.4852	0.8597	0.8597	0.0418	0.0403	0.1493	0.013	0.030	0.014	0.0031	0.0027	0.0020	0.7010	
2.008	4.05			0.4813	0.4888	0.8740	0.8608	0.0399	0.0486	0.1375	0.014	0.034	0.014	0.0033	0.0035	0.0020	0.7102	
2.008	6.00			0.5004	0.4711	0.8657	0.8509	0.0461	0.0504	0.1778	0.013	0.032	0.015	0.0032	0.0031	0.0020	0.7105	
2.008	6.00			0.4787	0.4693	0.8564	0.8419	0.0466	0.0474	0.1807	0.012	0.030	0.015	0.0029	0.0029	0.0020	0.7193	
2.008	6.00			0.4855	0.4725	0.8543	0.8366	0.0467	0.0644	0.1793	0.012	0.031	0.015	0.0030	0.0028	0.0020	0.7270	
2.005	10.00			0.5012	0.4815	0.8229	0.8060	0.1030	0.1745	0.2925	0.009	0.022	0.017	0.0027	0.0030	0.0021	0.7333	
2.005	10.00			0.5009	0.4779	0.8174	0.7791	0.0884	0.1855	0.2941	0.010	0.021	0.017	0.0028	0.0028	0.0021	0.7340	
2.003	9.95			0.4873	0.4831	0.8073	0.7791	0.0710	0.1376	0.2932	0.009	0.020	0.017	0.0026	0.0026	0.0021	0.7340	
2.011	12.00			0.5075	0.4765	0.7726	0.7283	0.1180	0.2290	0.2783	0.014	0.024	0.016	0.0027	0.0028	0.0021	0.7340	
2.005	12.00			0.4926	0.4624	0.7889	0.7248	0.1263	0.2414	0.2733	0.011	0.019	0.016	0.0029	0.0028	0.0021	0.7340	
2.009	14.00			0.4845	0.4563	0.7795	0.6860	0.1083	0.2252	0.4609	0.011	0.019	0.014	0.0030	0.0030	0.0021	0.7340	
2.011	14.00			0.4852	0.4481	0.7474	0.6881	0.1066	0.2083	0.4698	0.011	0.015	0.014	0.0029	0.0025	0.0021	0.7340	
2.013	2.00	3		0.5129	0.4842	0.8670	0.8572	---	---	0.1280	0.014	0.029	0.014	0.0032	0.0030	0.0020	0.7017	
2.011	2.00			0.4879	0.4745	0.8783	0.8667	0.0597	0.0495	0.1323	0.014	0.034	0.014	0.0032	0.0035	0.0020	0.7080	
2.010	2.00			0.4918	0.4564	0.8686	0.8374	0.0546	0.0477	0.1336	0.011	0.034	0.013	0.0028	0.0031	0.0020	0.7197	
2.010	4.05			0.4965	0.4881	0.8338	0.8210	0.0689	0.0661	0.1502	0.014	0.021	0.014	0.0031	0.0023	0.0020	0.7064	
2.013	4.05			0.4739	0.4880	0.8892	0.8691	0.0561	0.0503	0.1518	0.014	0.035	0.014	0.0032	0.0026	0.0020	0.7215	
2.013	6.05			0.5197	0.4946	0.8854	0.8621	0.0507	0.0537	0.1787	0.014	0.030	0.015	0.0031	0.0030	0.0020	0.7215	
2.010	6.00			0.4644	0.4917	0.8838	0.8621	0.0536	0.0637	0.1881	0.013	0.032	0.014	0.0030	0.0030	0.0020	0.7270	
2.010	6.00			---	---	---	---	---	---	---	0.012	0.027	0.015	0.0030	0.0025	0.0020	0.7330	
2.010	1.95	2		---	---	---	---	---	---	---	0.014	0.028	0.013	0.0030	0.0018	0.0020	0.7017	
2.010	2.00			0.5045	0.4656	0.8991	0.8747	0.0502	0.0502	0.013	0.027	0.013	0.0031	0.0027	0.0020	0.704		
2.007	2.05			0.4818	0.4690	0.8462	0.8686	0.0547	0.0547	0.010	0.030	0.013	0.0030	0.0027	0.0020	0.7138		
2.010	2.00			---	---	---	---	---	---	---	0.013	0.032	0.013	0.0026	0.0026	0.0020	0.7215	
2.007	4.00			0.4990	0.4705	0.8624	0.8628	0.0540	0.0540	0.014	0.032	0.014	0.0030	0.0028	0.0020	0.7161		
2.010	4.00			0.4815	0.4773	0.8656	0.8624	0.0524	0.0524	0.014	0.034	0.014	0.0032	0.0028	0.0020	0.7183		
2.007	4.05			0.4804	0.4807	0.8640	0.8621	0.0633	0.0633	0.013	0.035	0.014	0.0031	0.0029	0.0020	0.7236		
2.008	3.95			0.4833	0.4802	0.8554	0.8522	0.0668	0.0668	0.013	0.030	0.014	0.0030	0.0029	0.0020	0.7310		
2.004	10.05			0.5269	0.4840	0.8443	0.8872	0.1119	0.1119	0.011	0.027	0.016	0.0029	0.0025	0.0020	0.7340		
1.834	2.00			0.4686	0.5067	0.8744	0.8349	0.0788	0.1025	0.011	0.026	0.016	0.0028	0.0029	0.0020	0.7340		
1.834	2.00			0.4258	0.4595	0.8318	0.8243	---	---	0.012	0.024	0.014	0.0028	0.0028	0.0020	0.7340		
1.836	2.05			0.4387	0.4295	0.8725	0.8428	0.0774	0.0677	0.010	0.028	0.014	0.0024	0.0022	0.0020	0.7340		
1.831	4.00			0.4136	0.4605	0.8954	0.8719	0.0977	0.1032	0.012	0.024	0.014	0.0024	0.0023	0.0021	0.7338		
1.834	4.00			0.4535	0.4575	0.8982	0.8731	0.0920	0.0991	0.011	0.028	0.014	0.0027	0.0022	0.0021	0.7340		
1.837	4.00			0.4157	0.4523	0.8888	0.8671	0.0656	0.0813	0.008	0.026	0.014	0.0025	0.0031	0.0021	0.7340		
1.839	6.00			---	---	---	---	---	---	---	0.011	0.023	0.015	0.0020	0.0025	0.0021	0.7340	
1.838	6.05			0.5505	0.4456	0.8879	0.8956	0.0758	0.1044	0.010	0.024	0.015	0.0026	0.0025	0.0022	0.7340		
1.836	8.00			0.4330	0.4390	0.8725	0.8514	0.0765	0.0849	0.010	0.024	0.015	0.0024	0.0025	0.0021	0.7340		
1.836	8.05			0.4458	0.4464	0.8446	0.8464	0.0930	0.1266	0.010	0.026	0.016	0.0024	0.0026	0.0022	0.7340		
1.836	8.05			0.4373	0.4486	0.8749	0.8419	0.0941	0.1155	0.010	0.022	0.016	0.0024	0.0029	0.0022	0.7340		
1.836	10.00			0.5227	0.4264	0.8296	0.8140	0.0842	0.0870	0.011	0.026	0.016	0.0024	0.0025	0.0022	0.7340		
0.882	2.00			0.1985	0.1996	0.9909	0.9818	0.0176	0.0178	0.011	0.024	0.015	0.0036	0.0044	0.0029	0.6770		
0.885	2.05			0.2003	0.1997	0.9904	0.9814	0.0191	0.0178	0.012	0.024	0.015	0.0037	0.0044	0.0029	0.7102		
0.883	2.00			0.2072	0.2033	0.9888	0.9815	0.0202	0.0203	0.011	0.025	0.015	0.0037	0.0045	0.0029	0.7340		
0.886	2.00			0.1990	0.1961	0.9909	0.9802	0.0201	0.0204	0.005	0.025	0.015	0.0024	0.0046	0.0029	0.7340		
0.887	4.00			---	---	---	---	---	---	0.012	0.024	0.015	0.0041	0.0044	0.0031	0.7338		
0.881	6.00			---	---	---	---	---	---	0	0.042	0.023	---	---	---	0.0035	0.7338	
0.885	10.15			0.2234	0.2452	0.9893	0.9803	0.0227	0.0203	0.012	0.024	0.013	0.0049	0.0055	0.0034	0.7338		
0.880	13.10			0.2118	0.2145	0.9902	0.9812	0.0227	0.0152	0.015	0.026	0.013	0.0060	0.0065	0.0037	0.7338		
2.212	2.05			0.4343	0.4304	0.7510	0.7486	0.0664	0.0567	0.013	0.024	0.015	0.0023	0.0025	0.0017	0.6830		
2.212	2.05			0.4362	0.4314	0.7490	0.7466	0.0633	0.0568	0.013	0.026	0.015	0.0021	0.0025	0.0017	0.6770		
2.130	2.00			0.4394	0.4165	0.8661	0.8590	0.0771	0.0755	0.014	0.027	0.014	0.0032	0.0028	0.0019	0.6820		
2.130	2.00			0.4395	0.4248	0.8128	0.8123	0.0614	0.0614	0.014	0.029	0.014	0.0031	0.0028	0.0019	0.6770		
2.122	2.00			0.4296	0.4276	0.8212	0.8222	0.0759	0.0546	0.014	0.026	0.014	0.0032	0.0026	0.001			



0317120000000000  
CONFIDENTIAL

CONFIDENTIAL  
DECLASSIFIED

25



A-23048

Figure 1.- Photograph of model in tunnel.

CONFIDENTIAL

CONFIDENTIAL

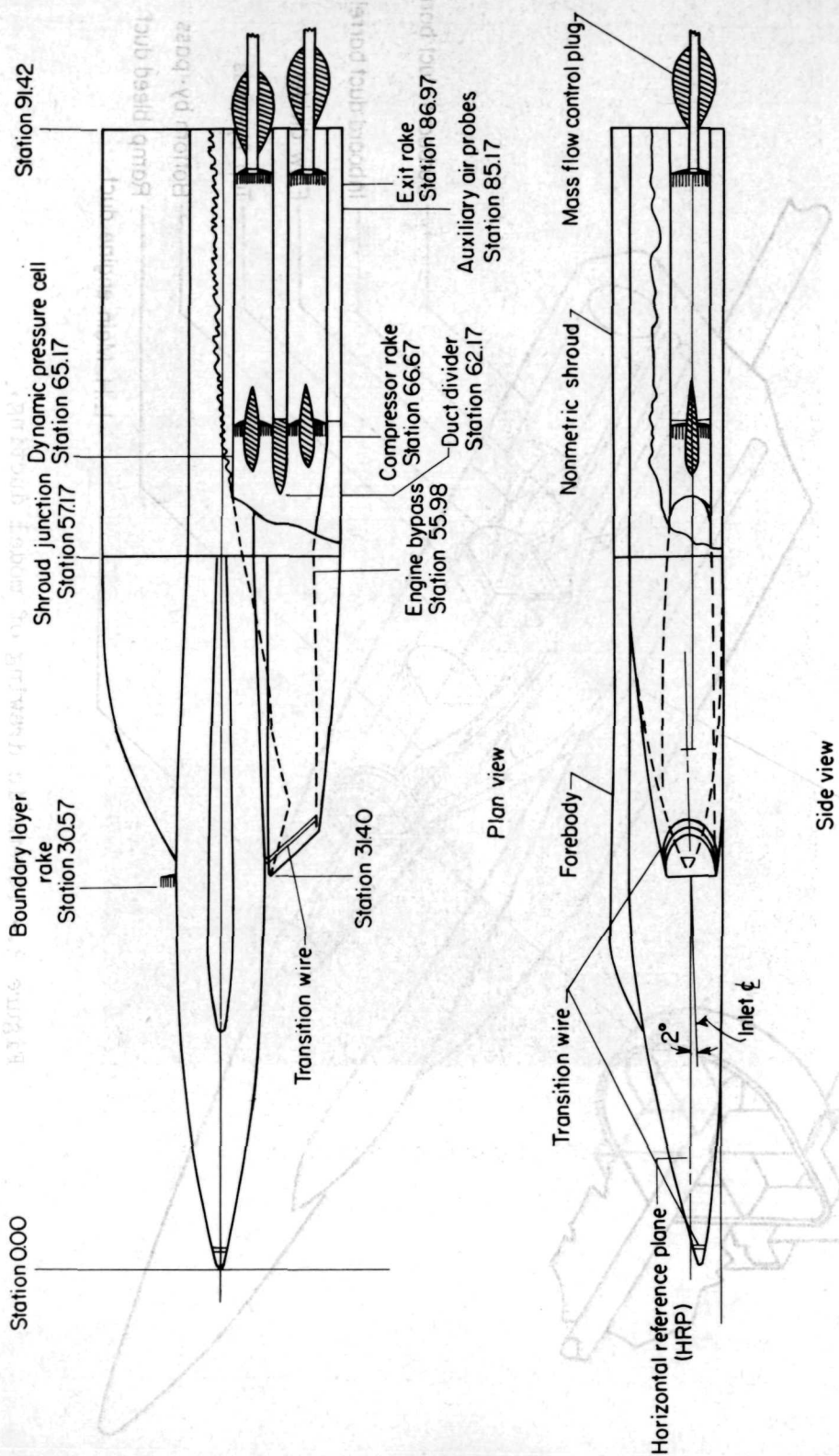


Figure 2.- Schematic diagram of model.

CONFIDENTIAL

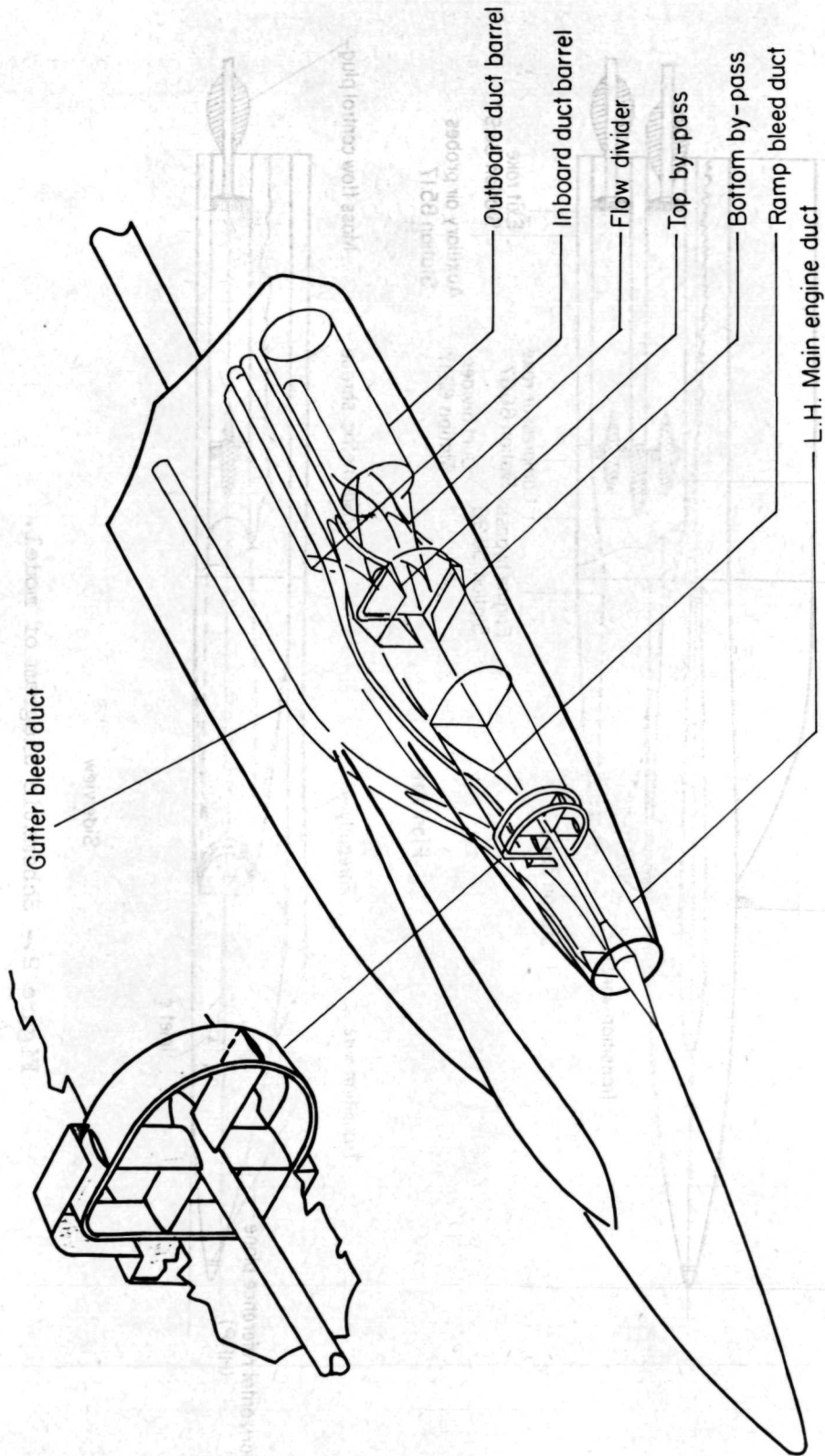
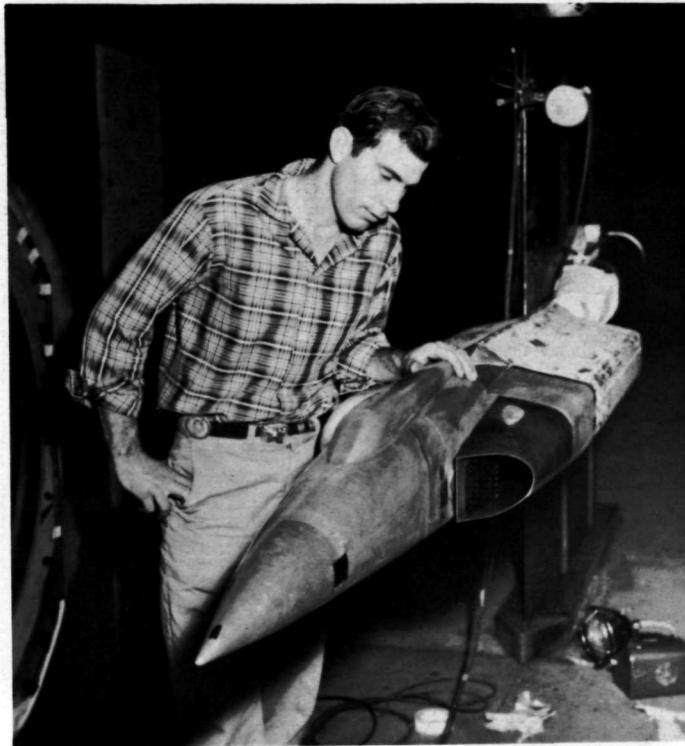


Figure 3.- Schematic drawing of model ducting.

CONFIDENTIAL



(a) Basic inlet.

A-23129



(b) Hooded inlet.

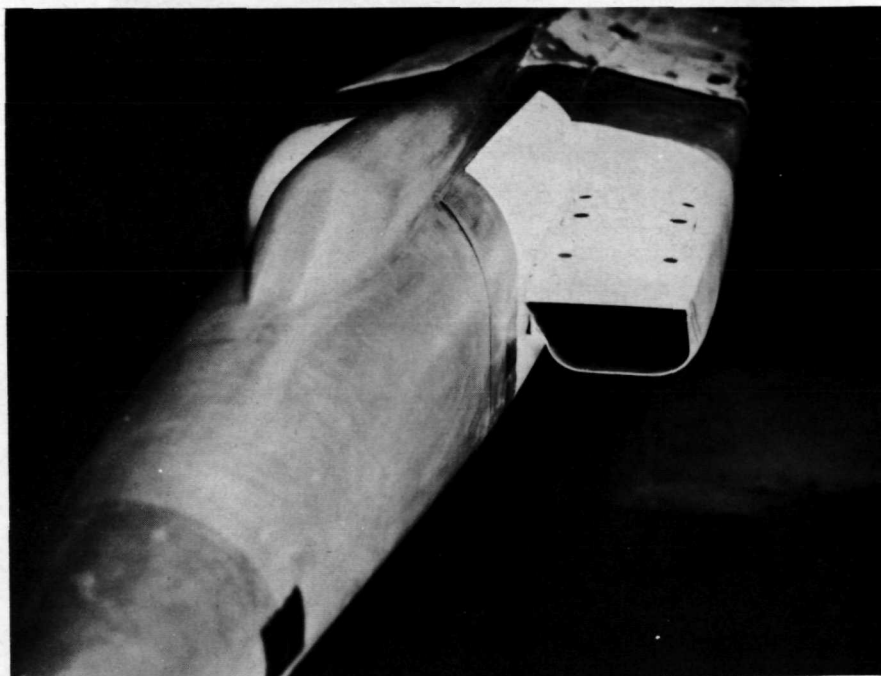
A-23127

Figure 4.- Photographs of inlet models.

CONFIDENTIAL

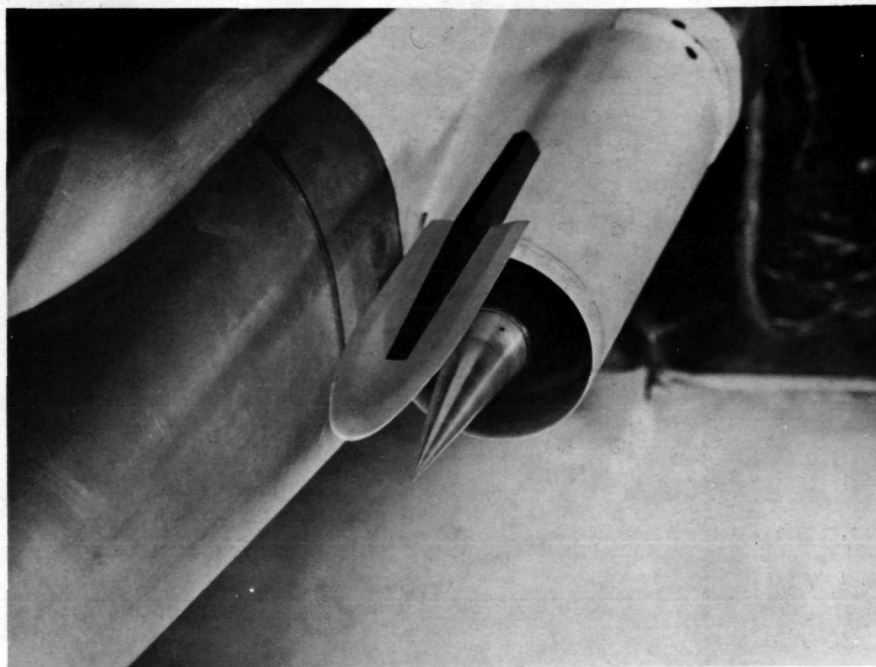
DECLASSIFIED

29



A-23150

(c) Horizontal ramp inlet.



A-23242

(d) Internal compression inlet.

Figure 4.- Concluded.

CONFIDENTIAL



CONFIDENTIAL

Body station 46.17

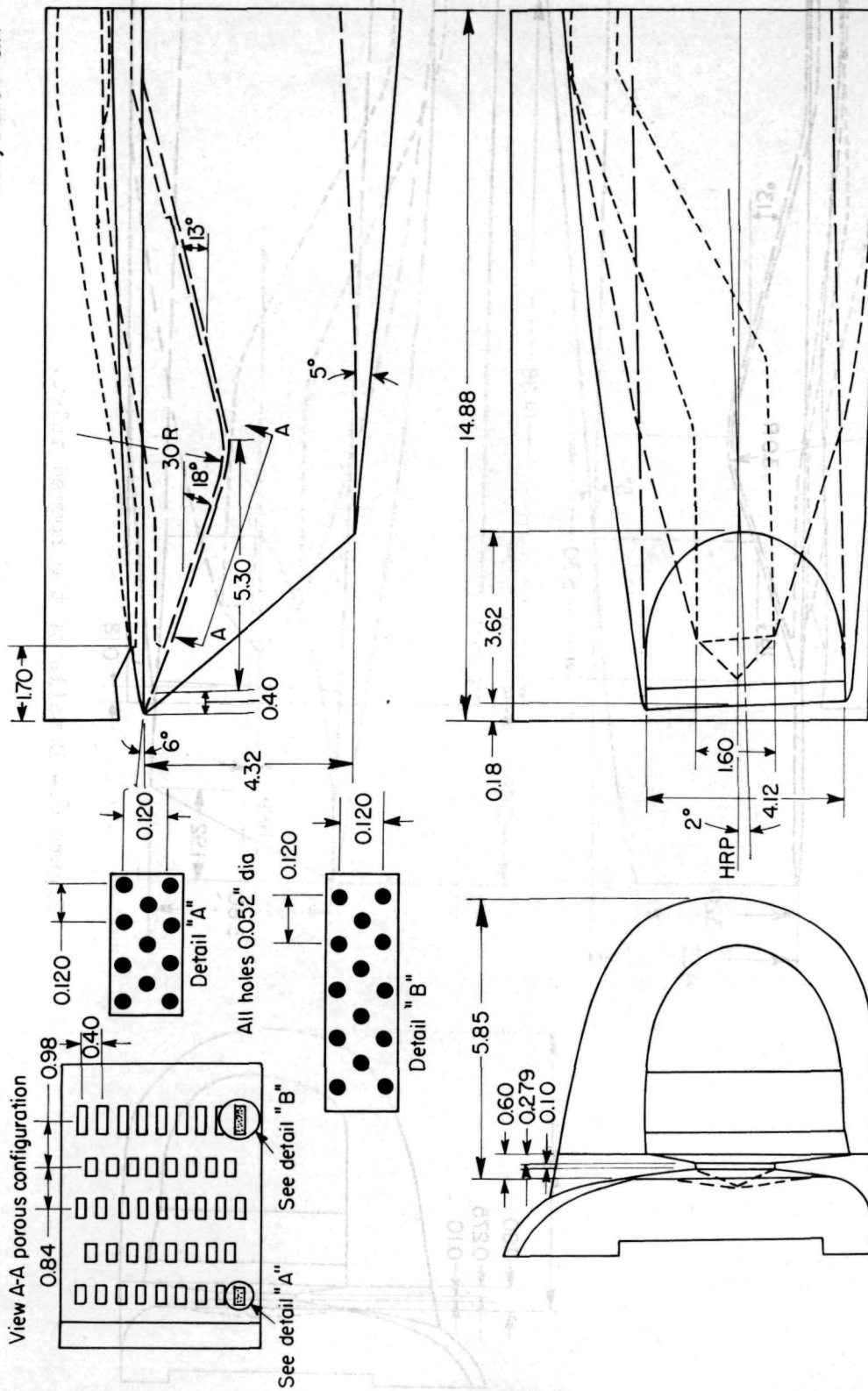


Figure 5.- Details of the basic inlet.

CONFIDENTIAL

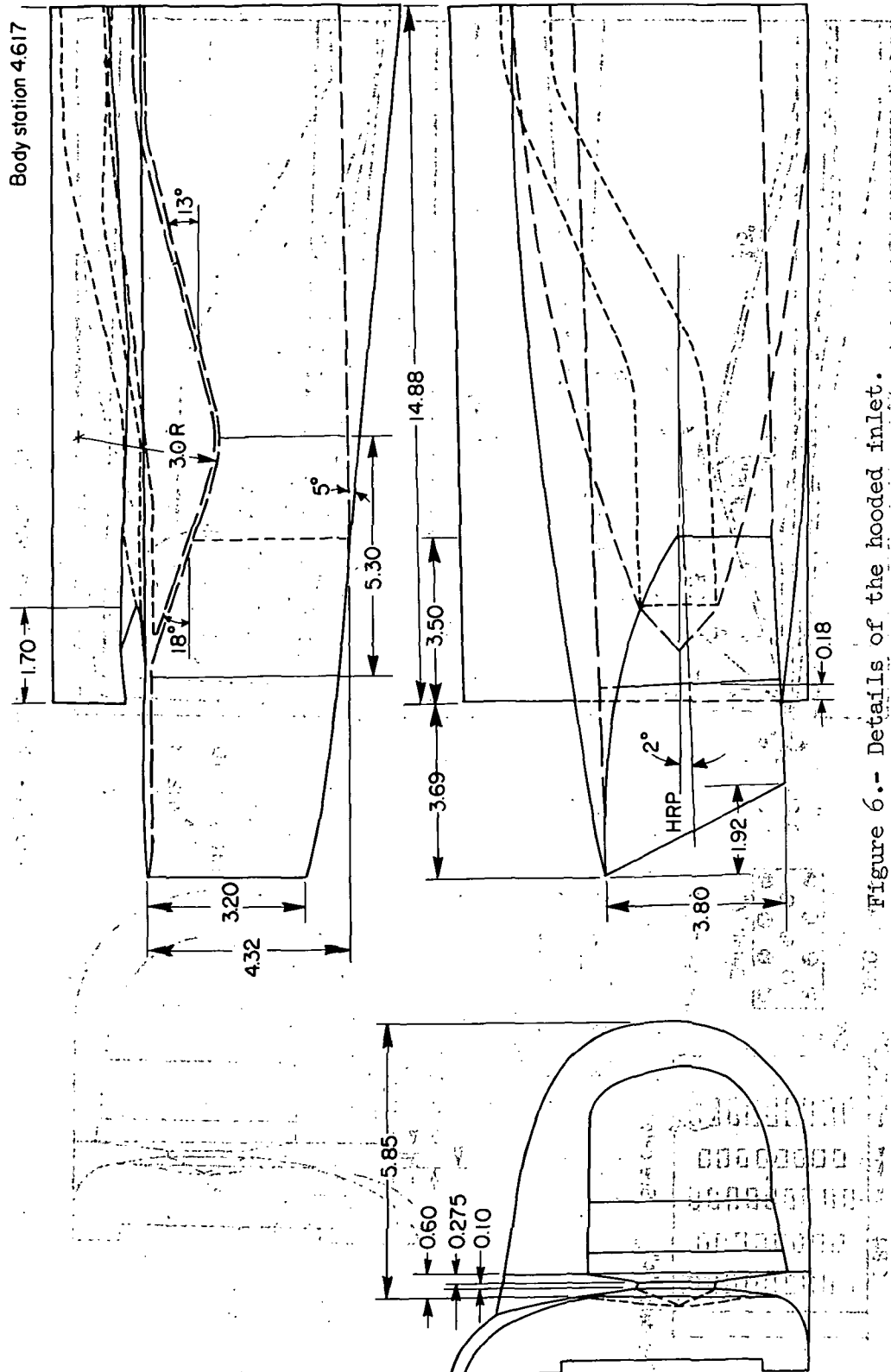
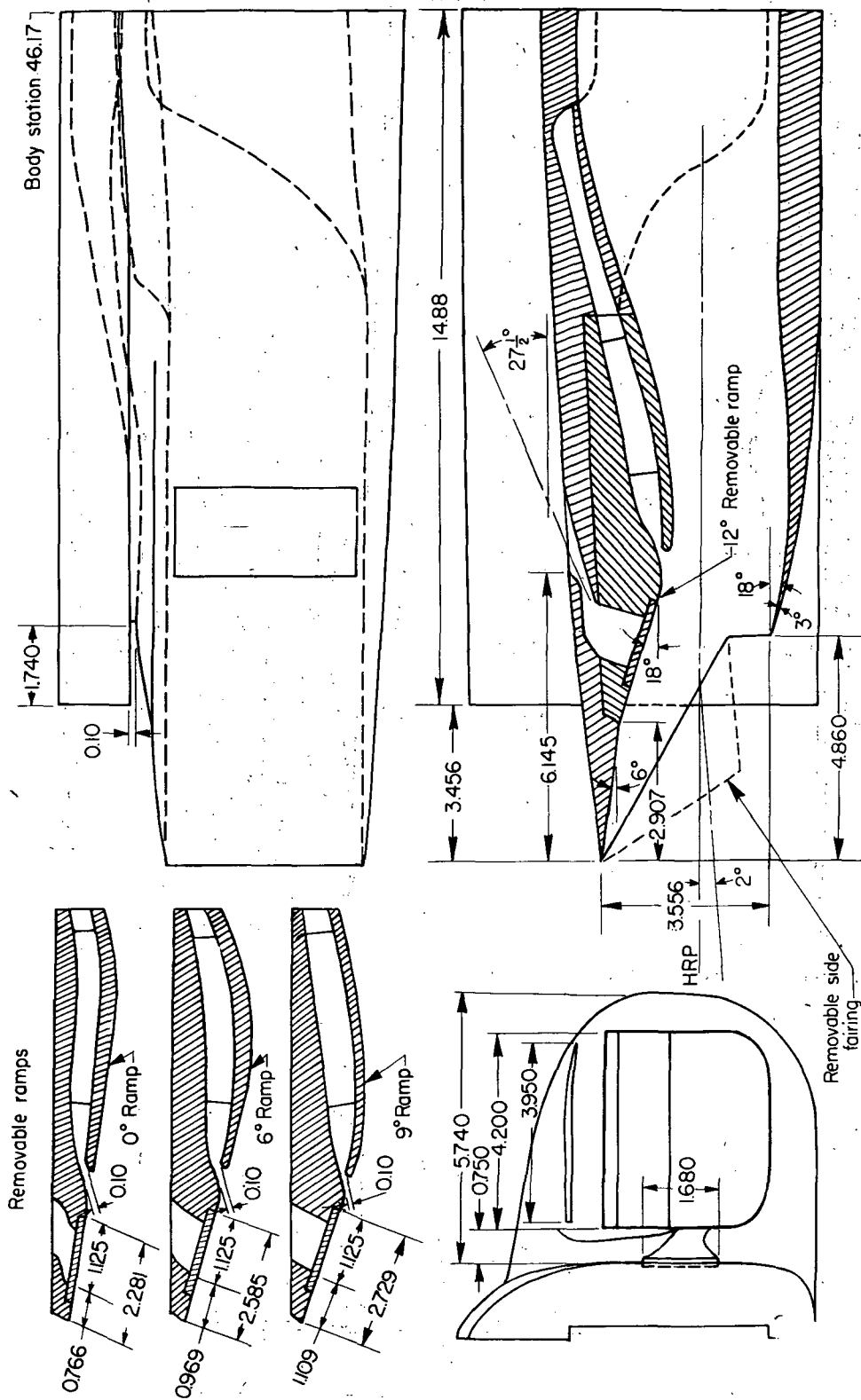


Figure 6.- Details of the hooded inlet.



CONFIDENTIAL

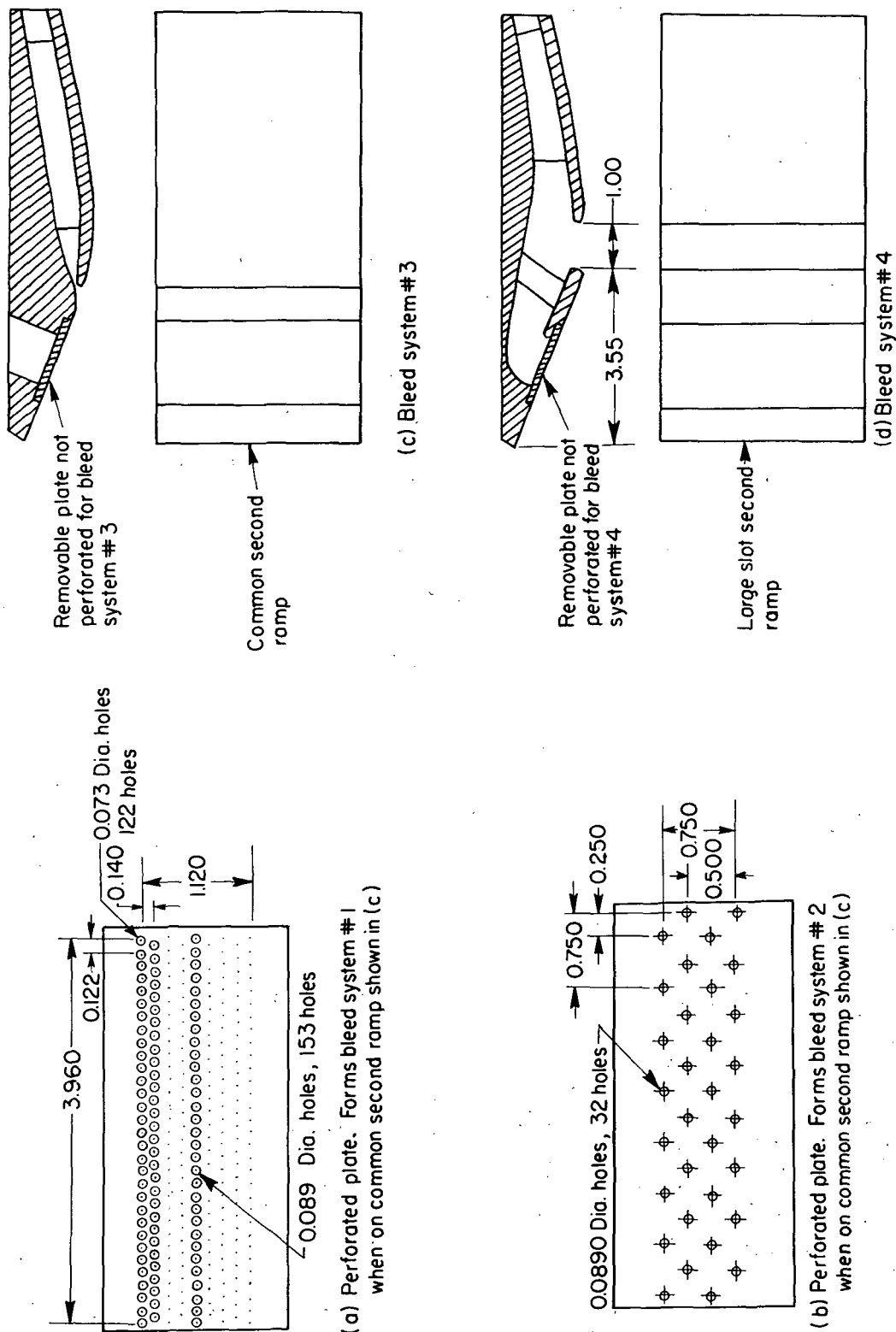


(a) Details of the inlet.

Figure 7.- Horizontal ramp inlet.

CONFIDENTIAL

CONFIDENTIAL

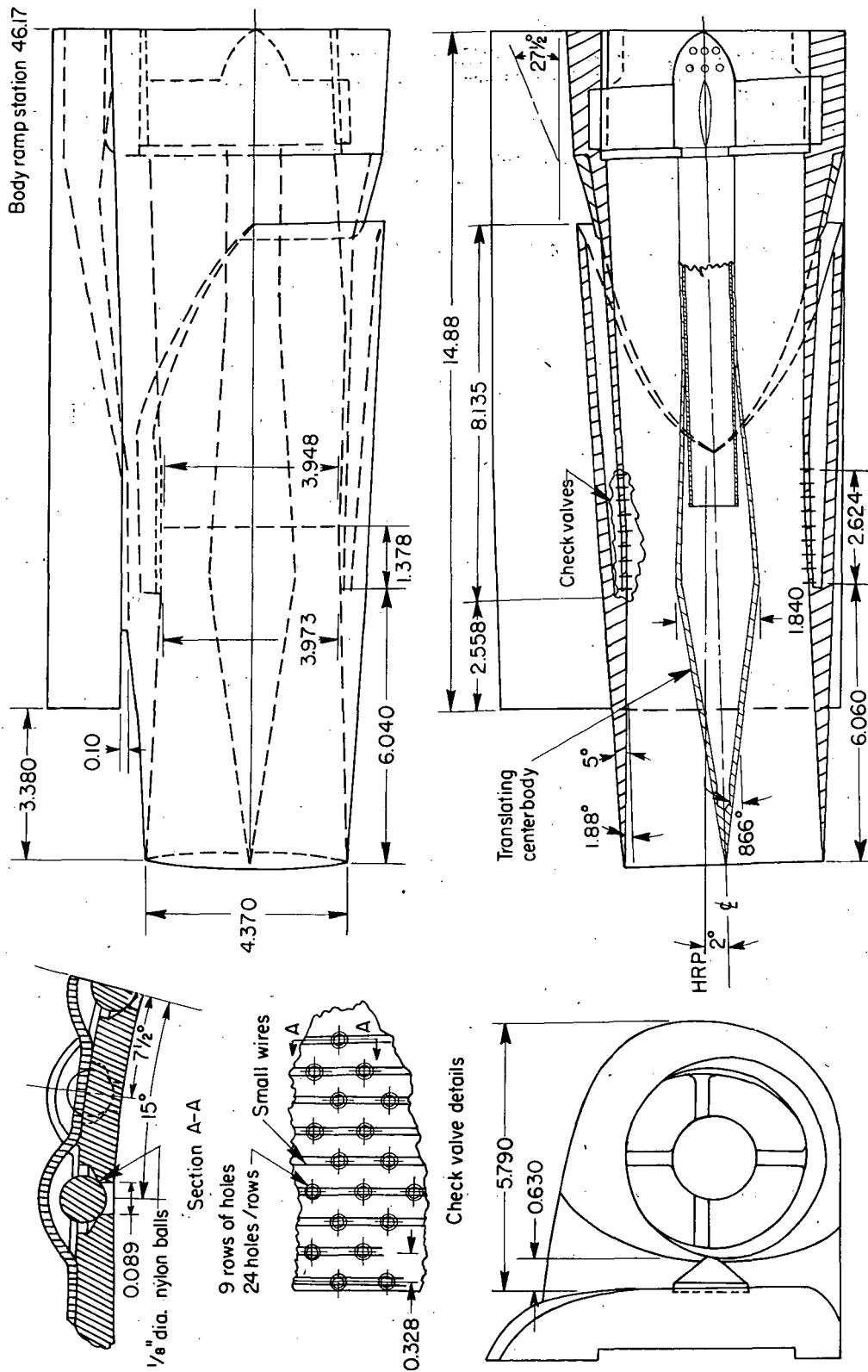


(b) Details of perforated ramps.

Figure 7.- Concluded.

CONFIDENTIAL

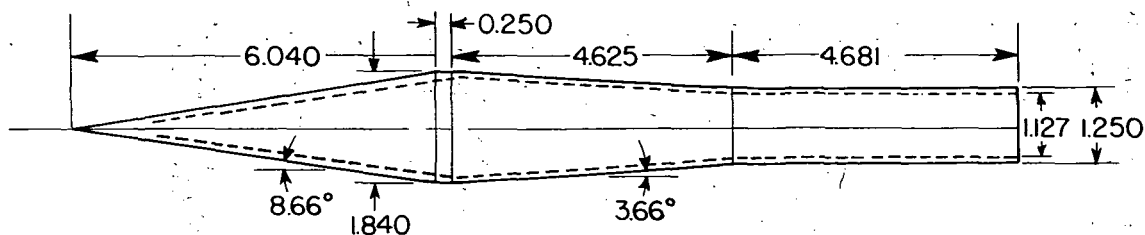
CONFIDENTIAL



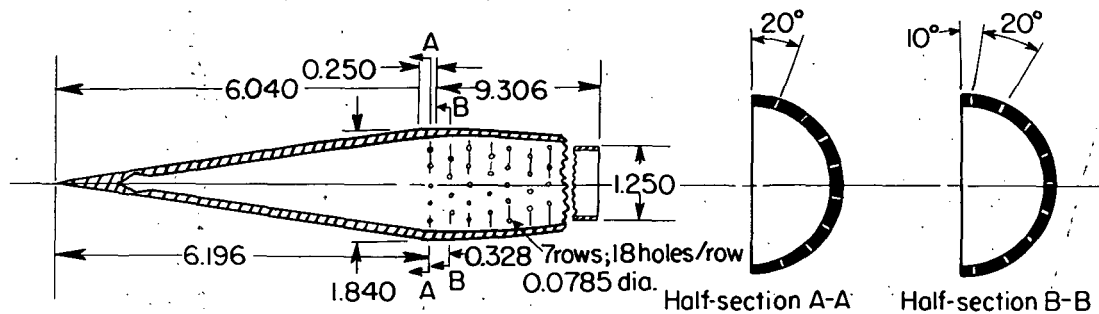
(a) Details of the inlet.

Figure 8.- Internal compression inlet.

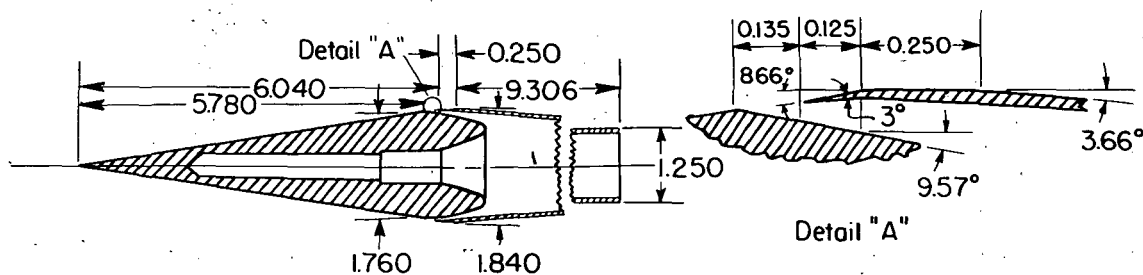
CONFIDENTIAL



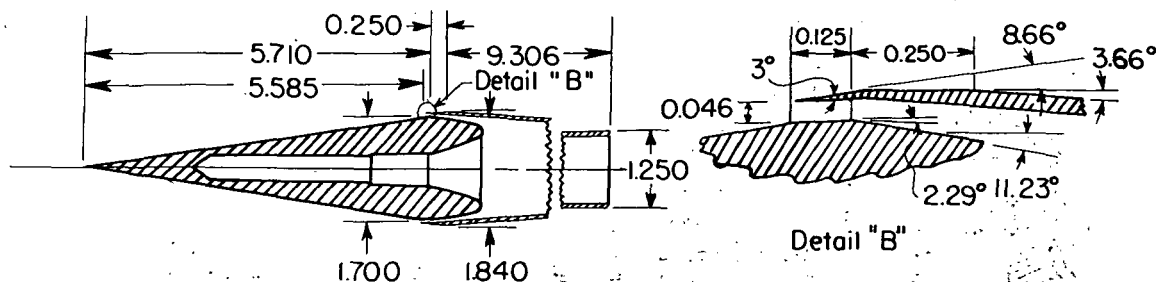
(a) Basic internal-compression inlet centerbody



(b) Perforated centerbody - Bleed configuration #1



(c) Centerbody with slot - Bleed configuration #2

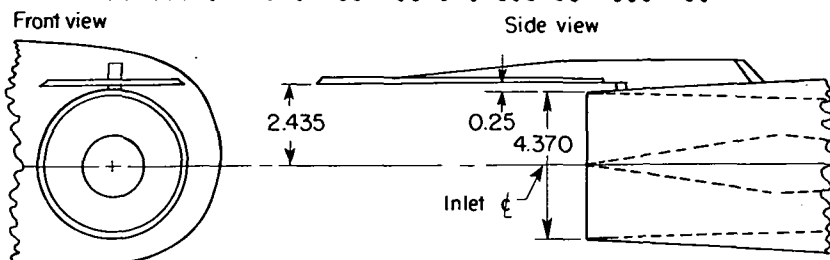


(d) Centerbody with scoop - Bleed configuration #3

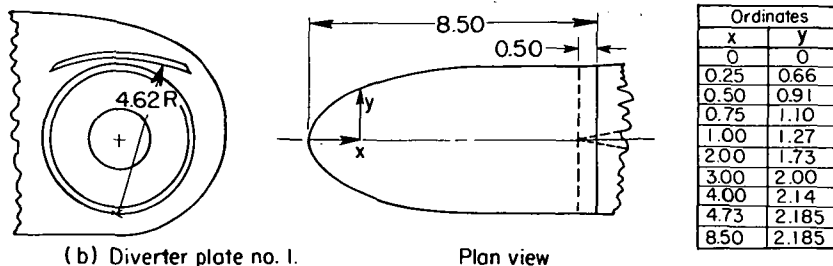
(b) Details of the centerbody bleed.

Figure 8.- Continued.

CONFIDENTIAL

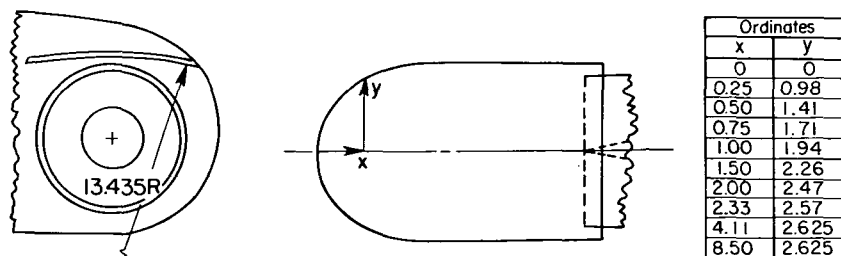


(a) Internal compression inlet with flow diverter plate mounted

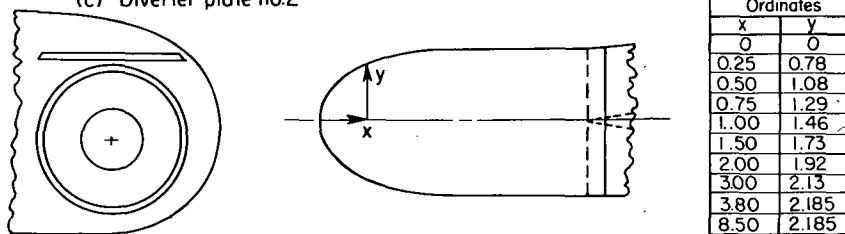


(b) Diverter plate no. 1.

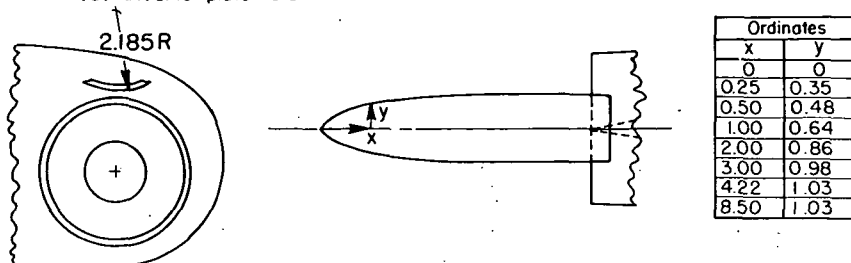
Plan view



(c) Diverter plate no.2



(d) Diverter plate no.3



(e) Diverter plate no.4

(c) Details of the flow deflector plates.

Figure 8.- Concluded.

CONFIDENTIAL

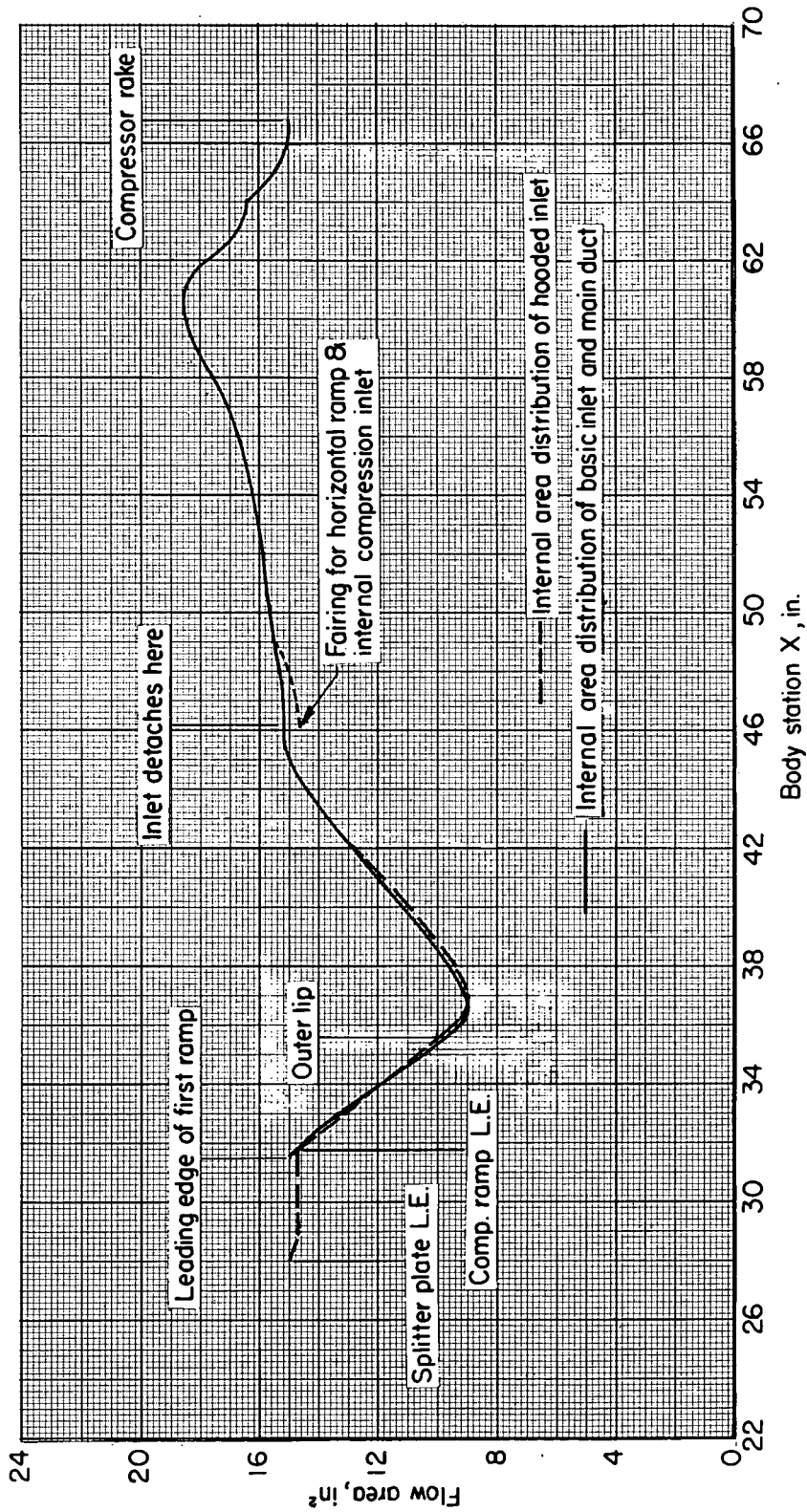


Figure 9.- Internal area distribution of basic inlet, hooded inlet, and main duct.

CONFIDENTIAL

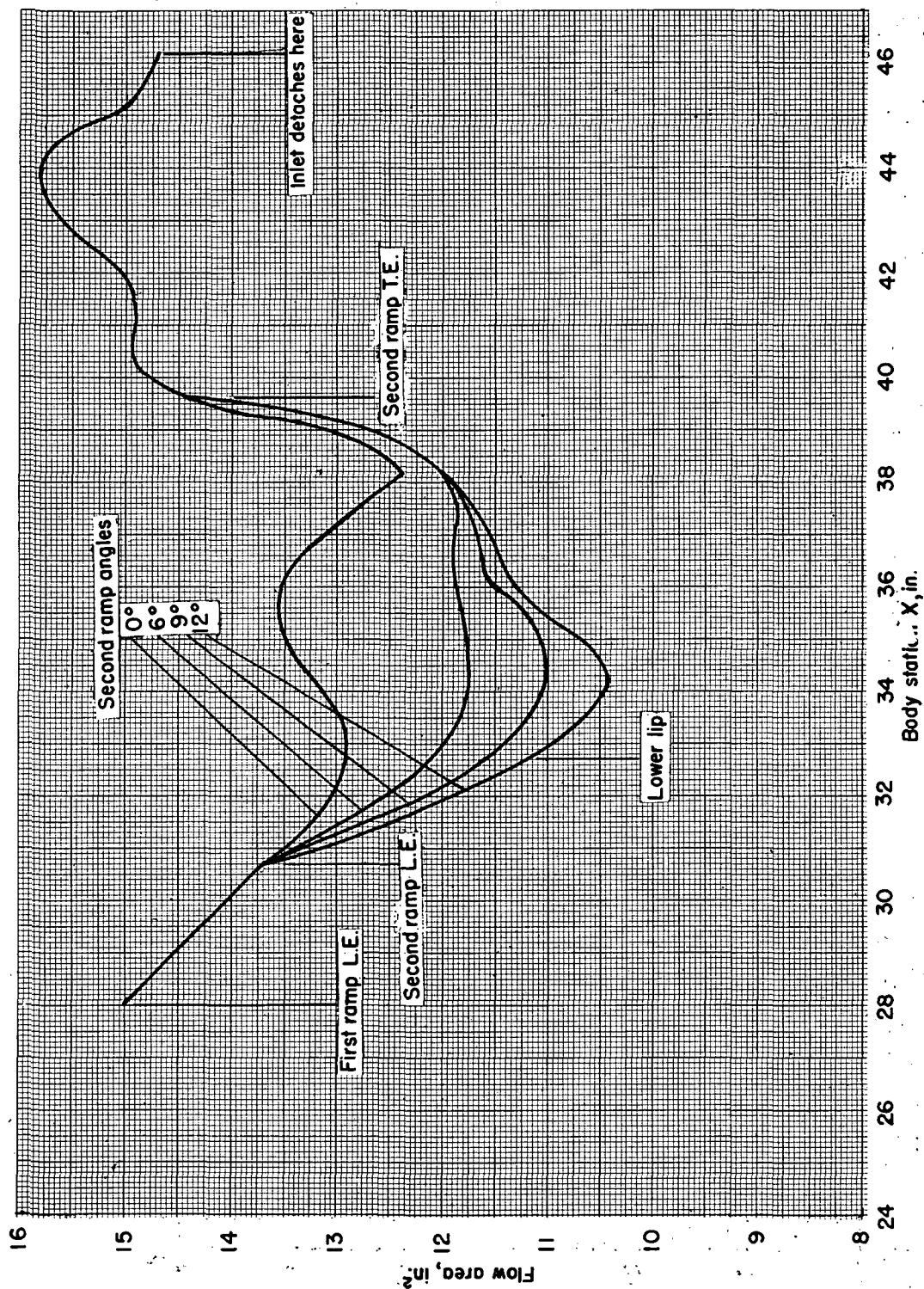


Figure 10.- Internal area distribution of horizontal ramp inlet.

CONFIDENTIAL

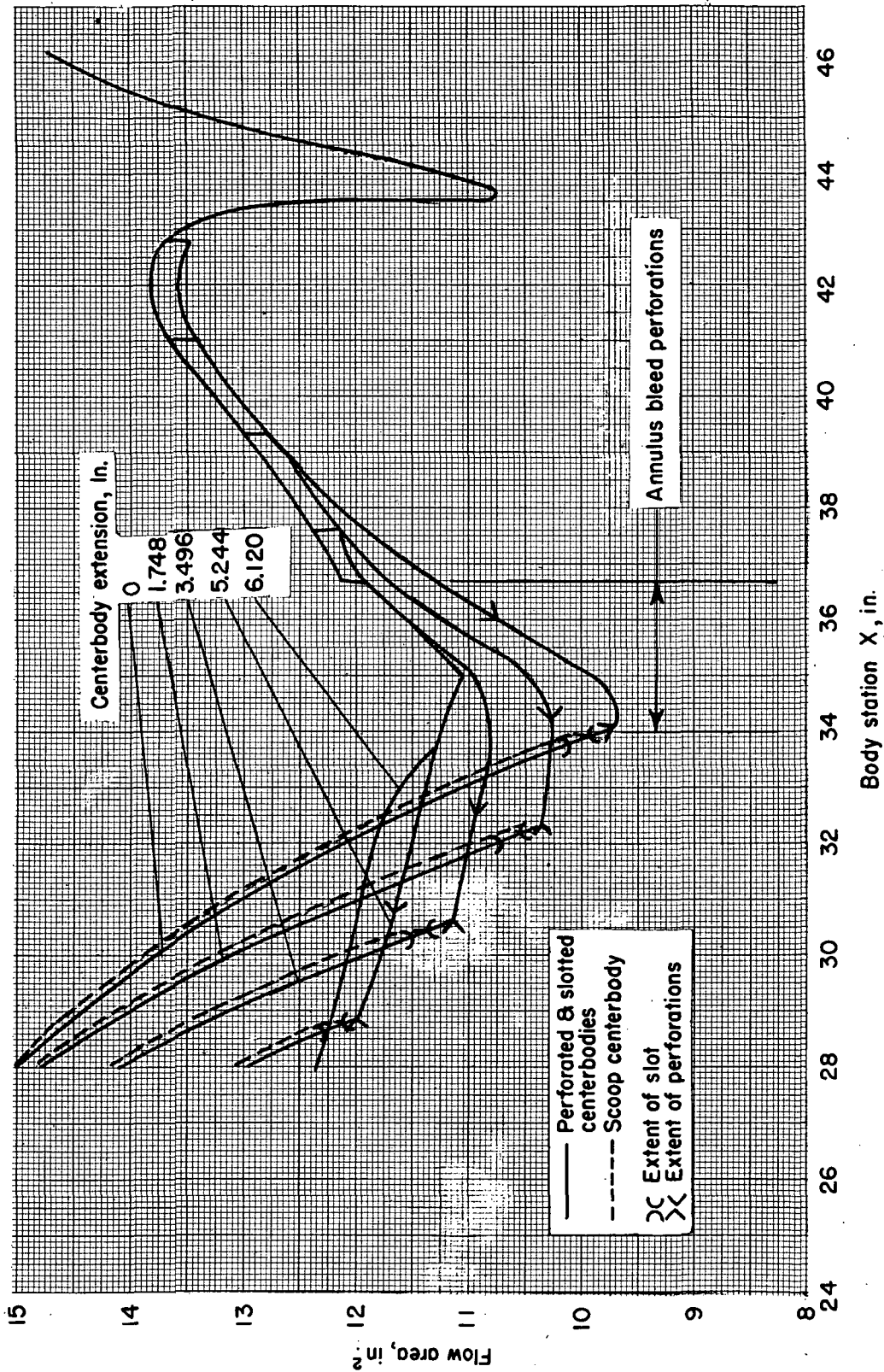


Figure 11.- Internal area distribution of internal compression inlet.



CONFIDENTIAL

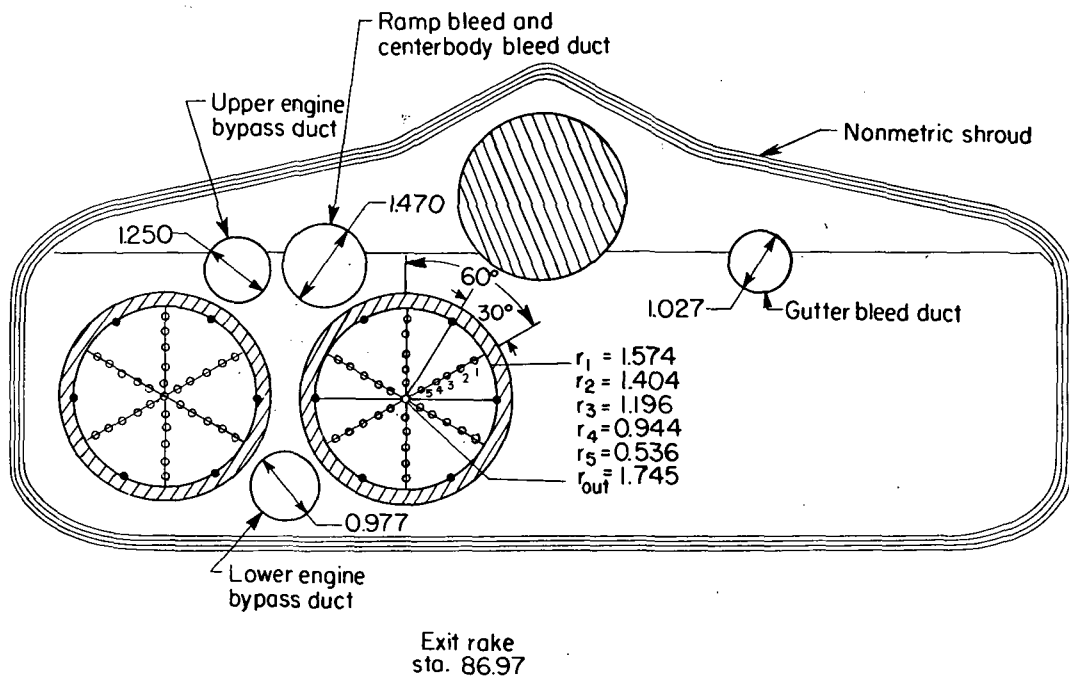
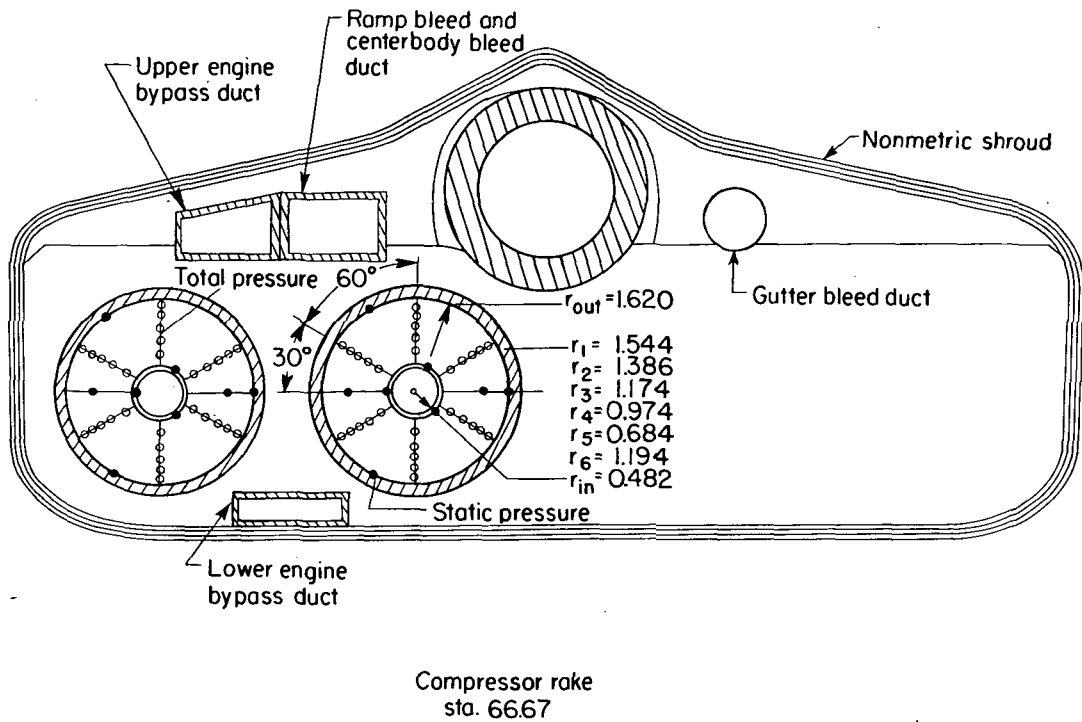


Figure 12.- Compressor and exit rake details.

CONFIDENTIAL

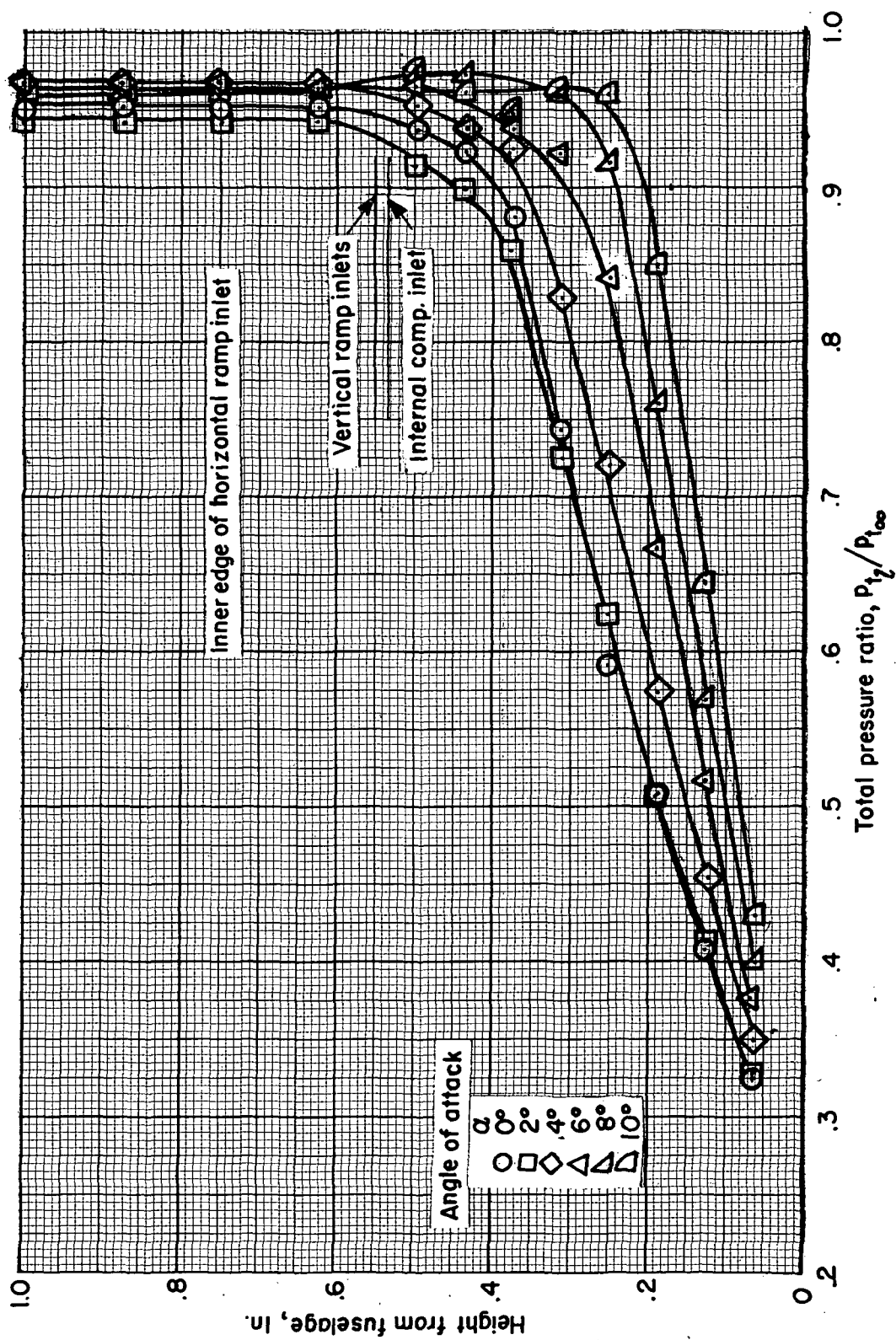


Figure 13.- Boundary-layer profiles, body station 30.57;  $M_\infty = 2.0$ .

CONFIDENTIAL

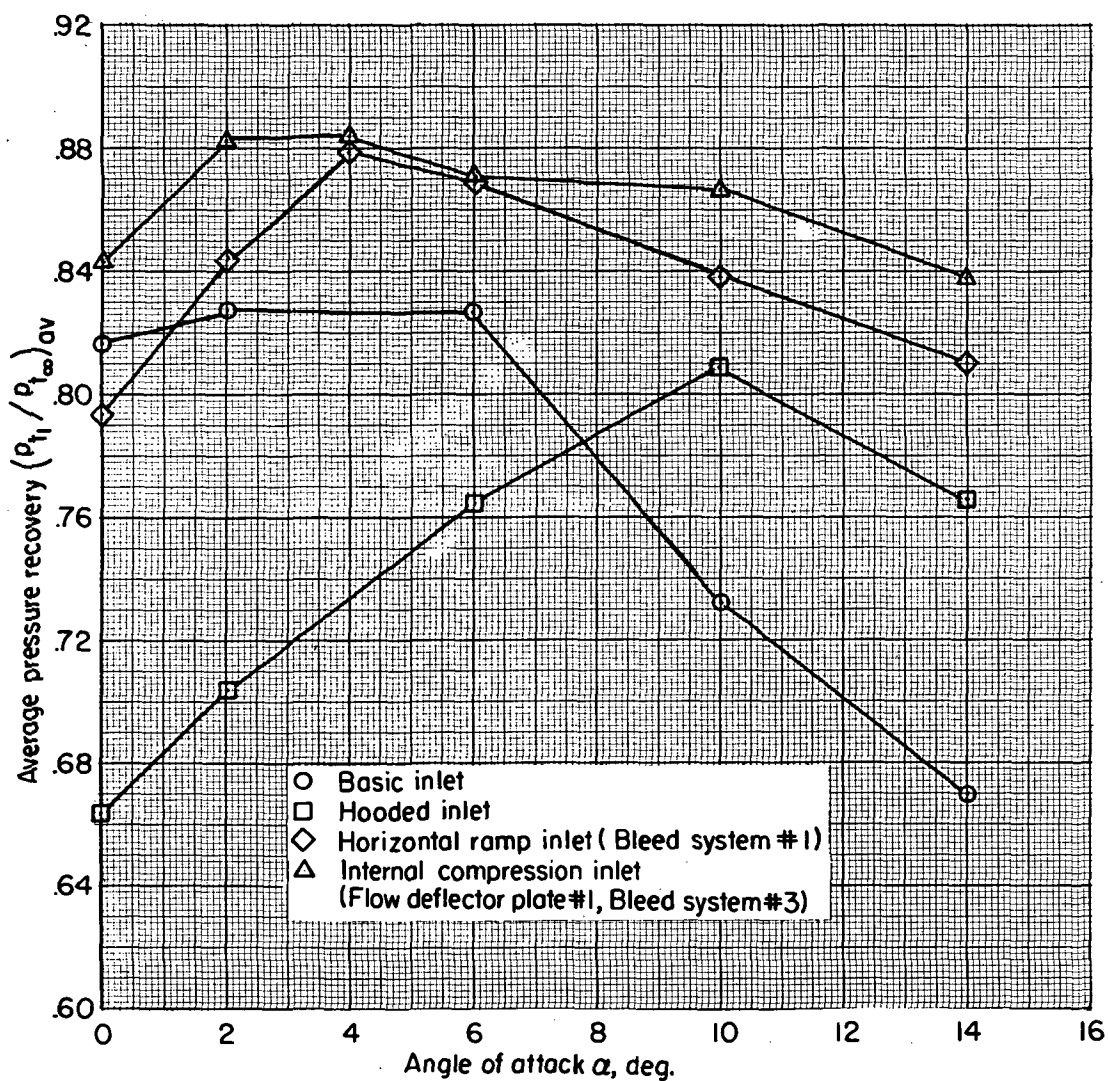
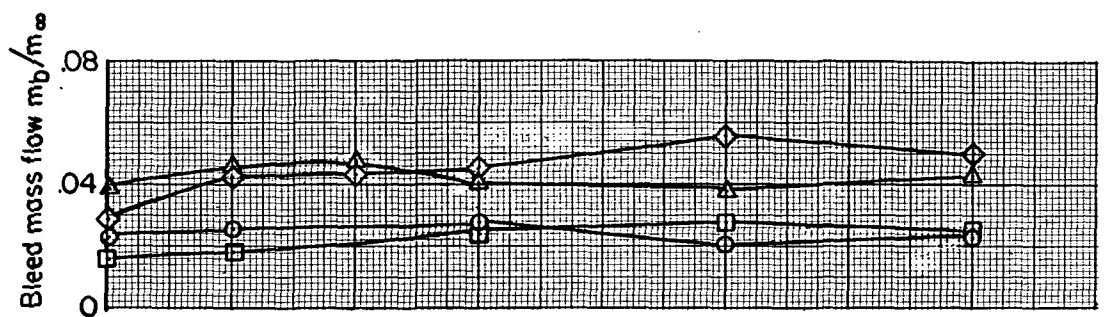


Figure 14.- Summary of best pressure recovery characteristics of inlets;  
 $M_\infty = 2.0$ .

CONFIDENTIAL

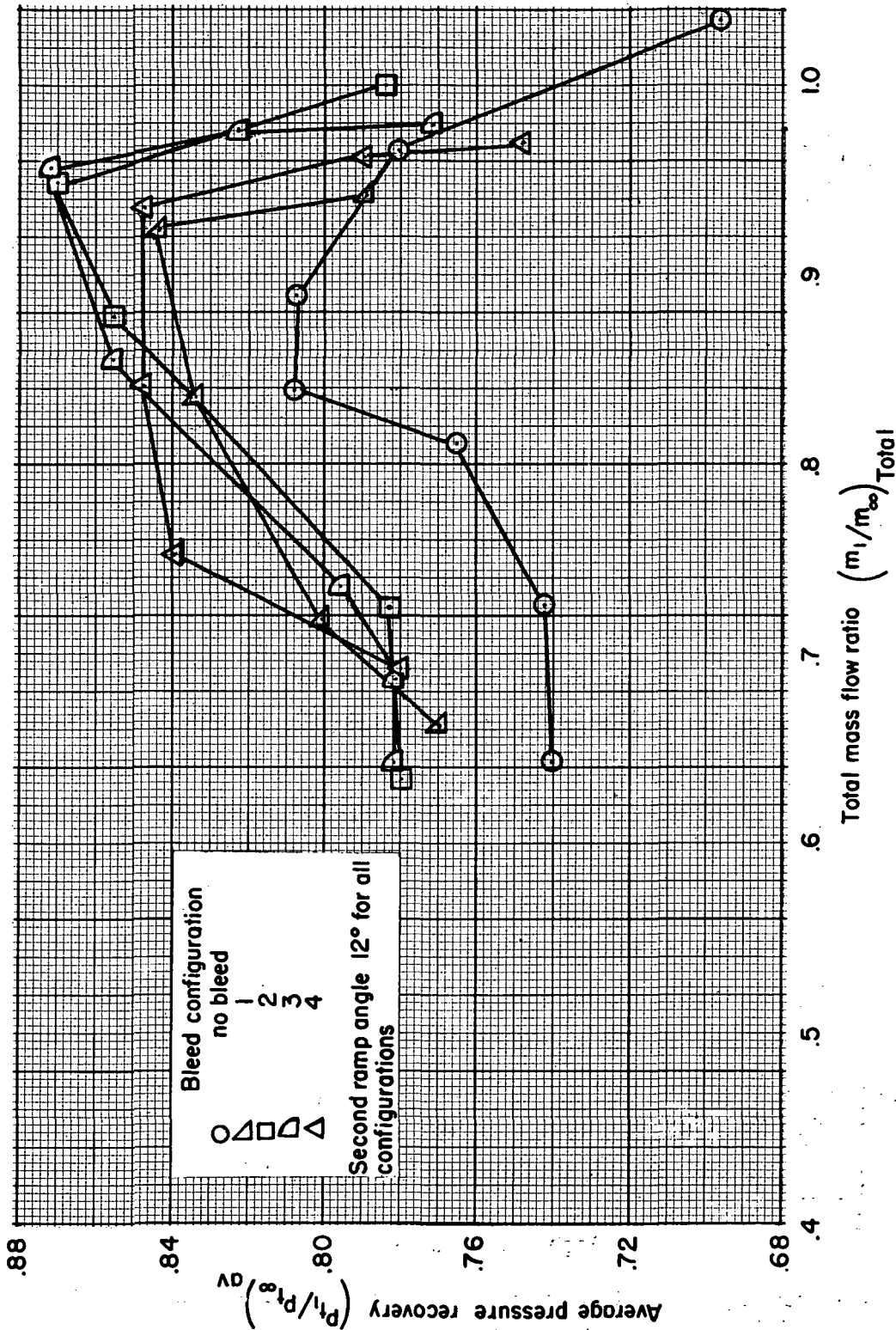


Figure 15.- Effect of bleed configuration on pressure recovery of horizontal ramp inlet;  
 $M_\infty = 2.0$ ,  $\alpha = 2.0^\circ$ .

CONFIDENTIAL

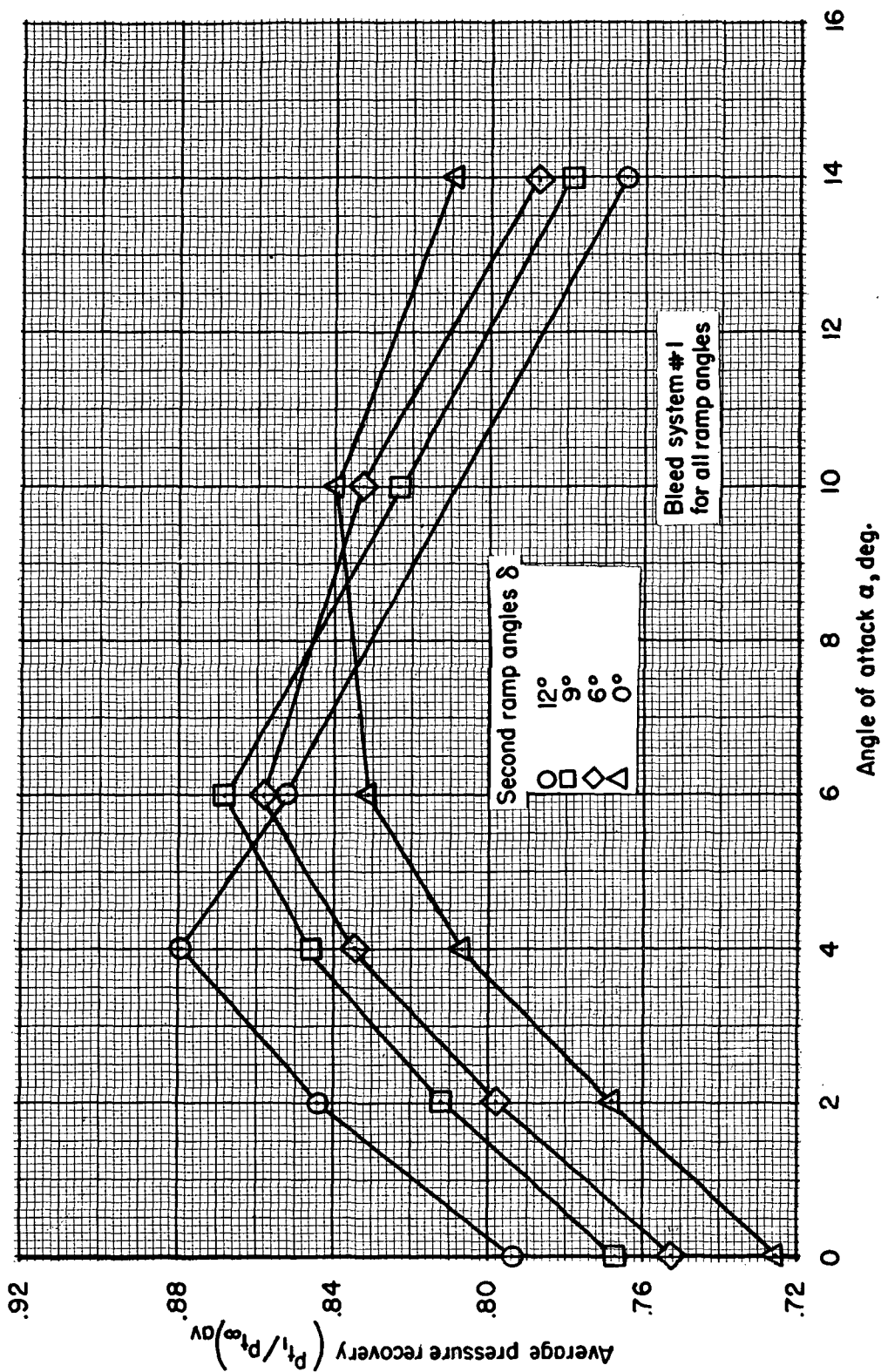


Figure 16.- Variation of pressure recovery for various second ramp angles of horizontal ramp inlet;  $M_\infty = 2.0$ .

CONFIDENTIAL

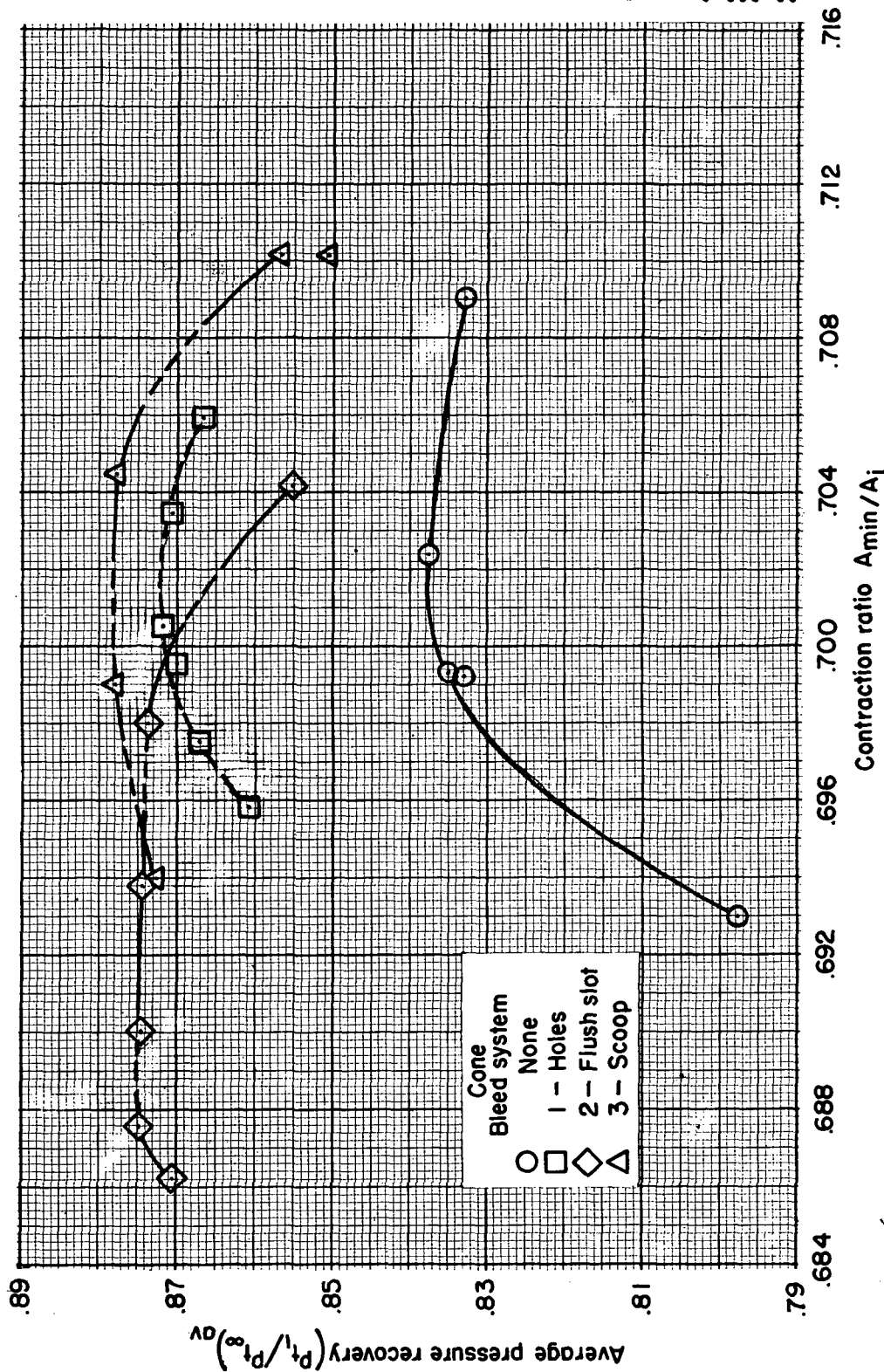


Figure 17.- Effect of centerbody bleed on pressure recovery of internal compression inlet;  
 $M_{\infty} = 2.0$ ,  $\alpha = 20^\circ$ .

CONFIDENTIAL

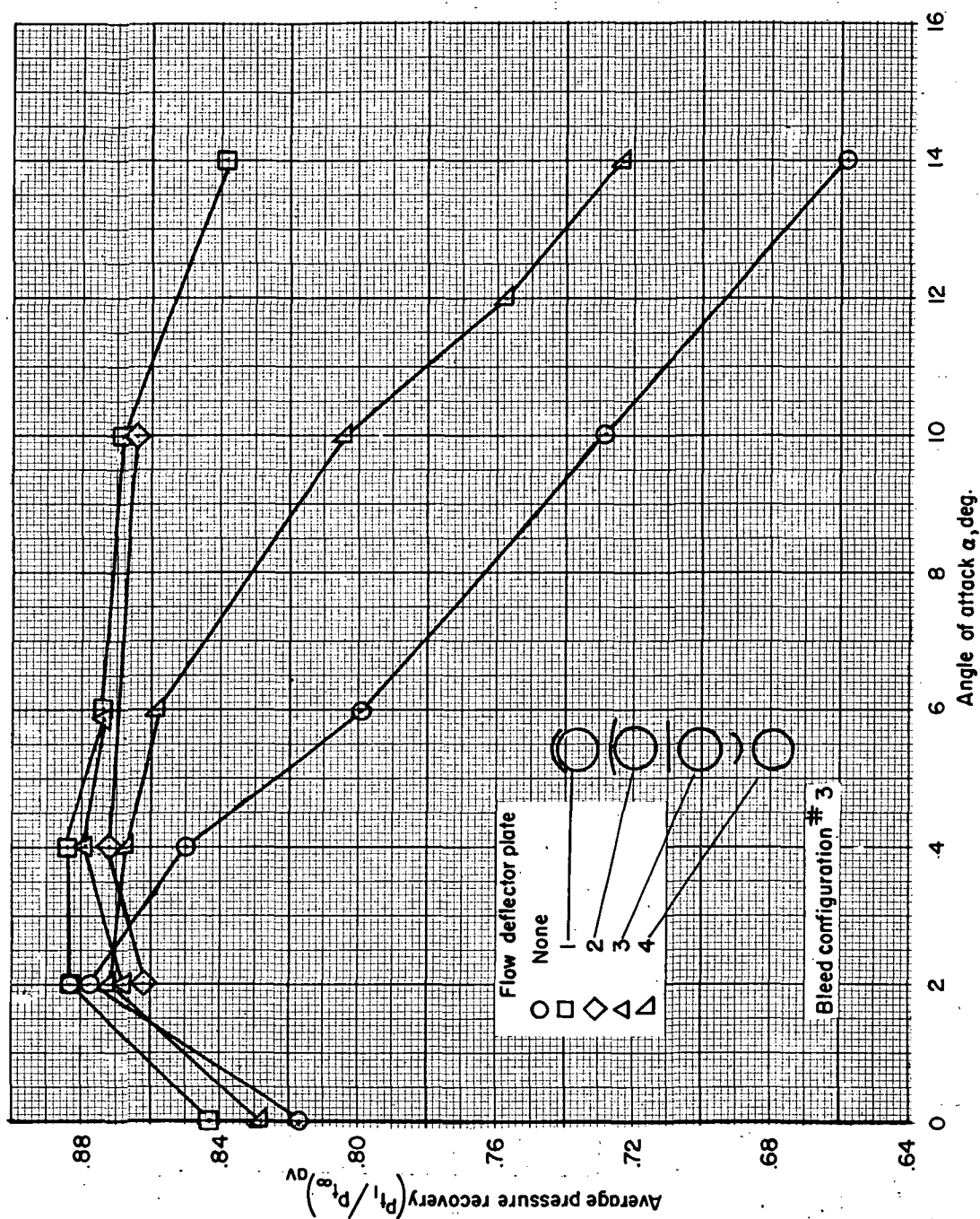


Figure 18.- Effect of flow deflector plate on pressure recovery of internal compression inlet;  $M_\infty = 2.0$ .

CONFIDENTIAL



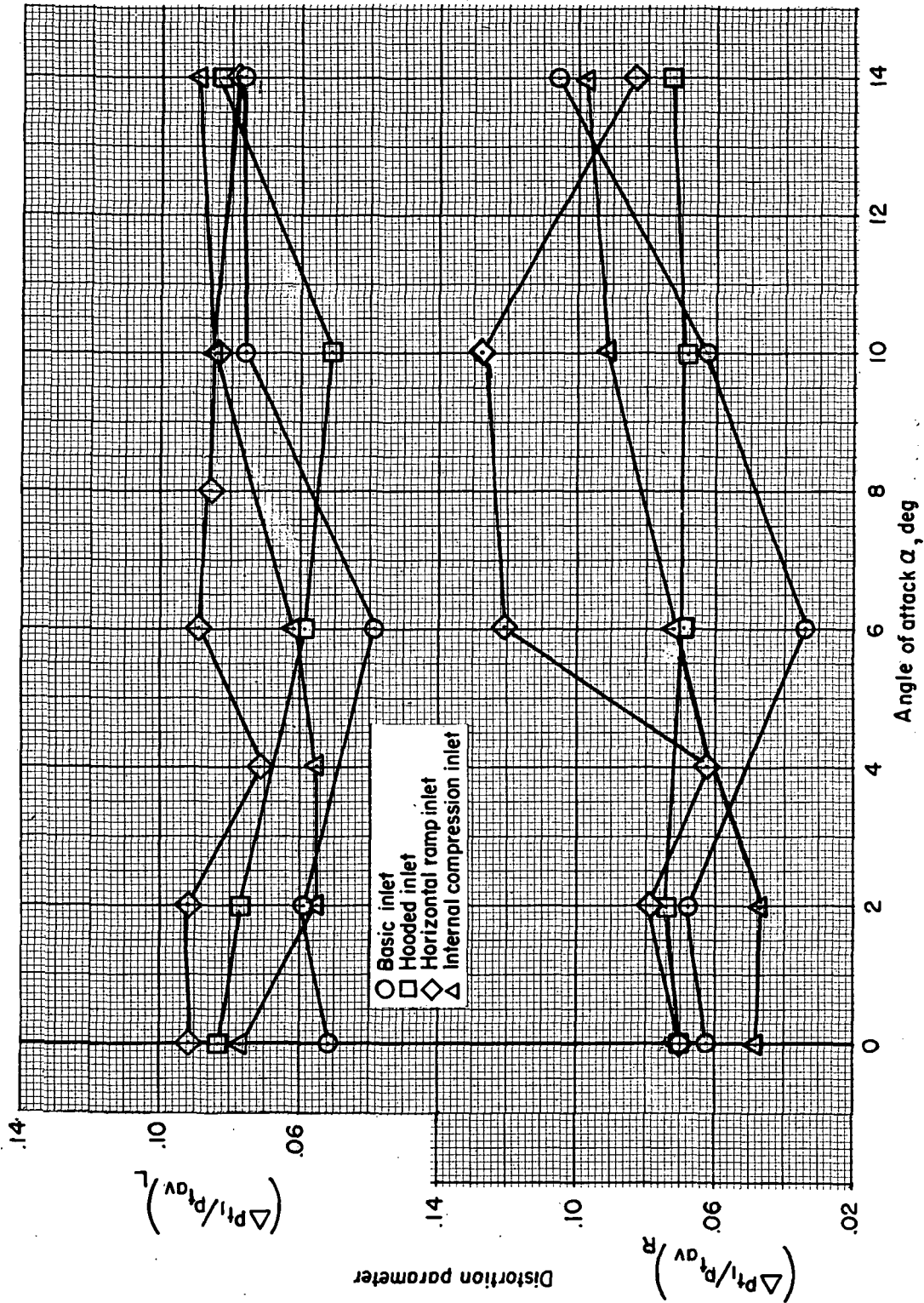


Figure 19.- Total pressure distortion at the compressor rake station;  $M_\infty = 2.0$ .



CONFIDENTIAL

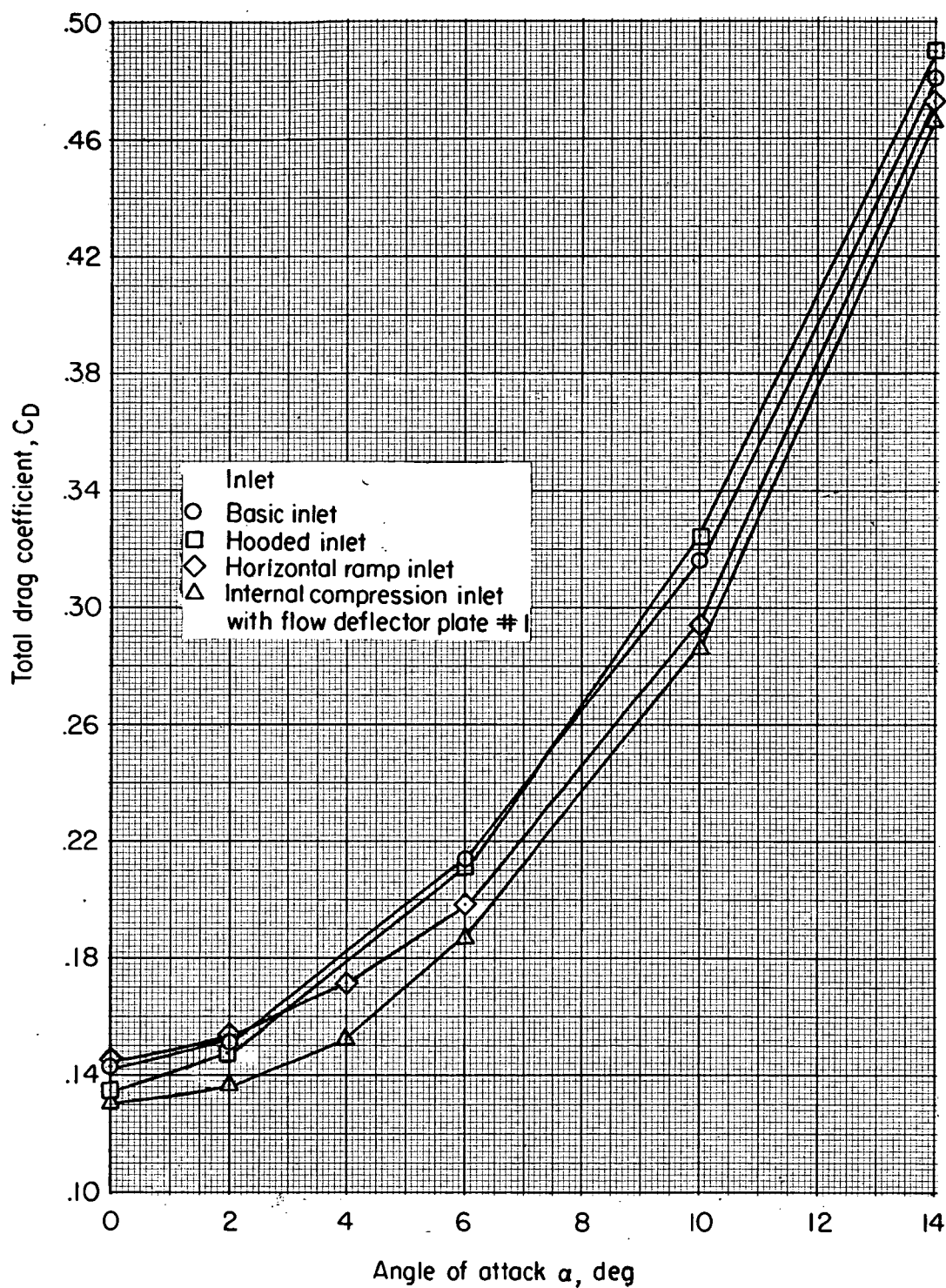


Figure 20.- Total drag coefficient for peak pressure recovery;  
 $M_\infty = 2.0$ .

CONFIDENTIAL

CONFIDENTIAL

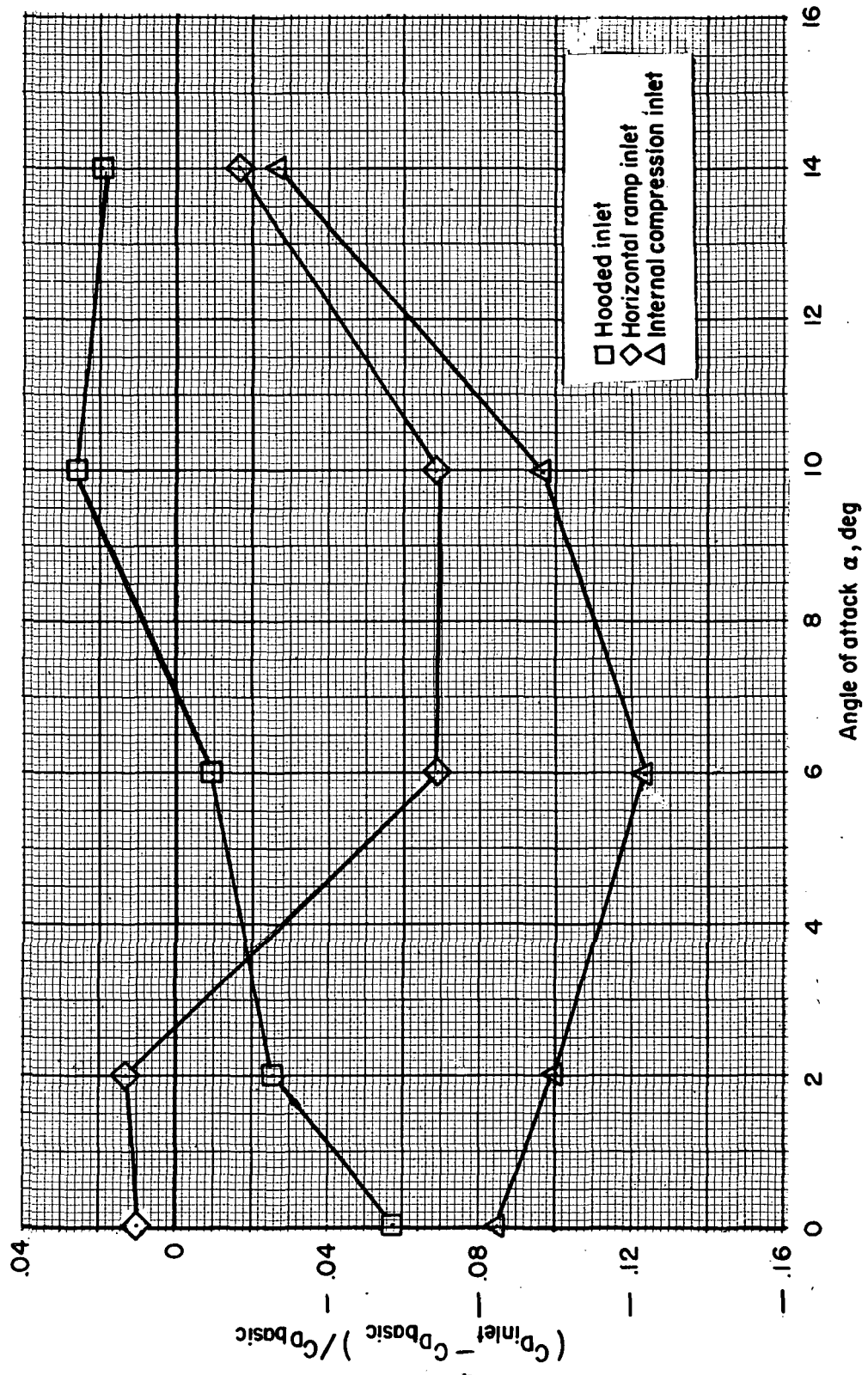


Figure 21.- Comparison of total drag for peak pressure recovery.

CONFIDENTIAL

CONFIDENTIAL

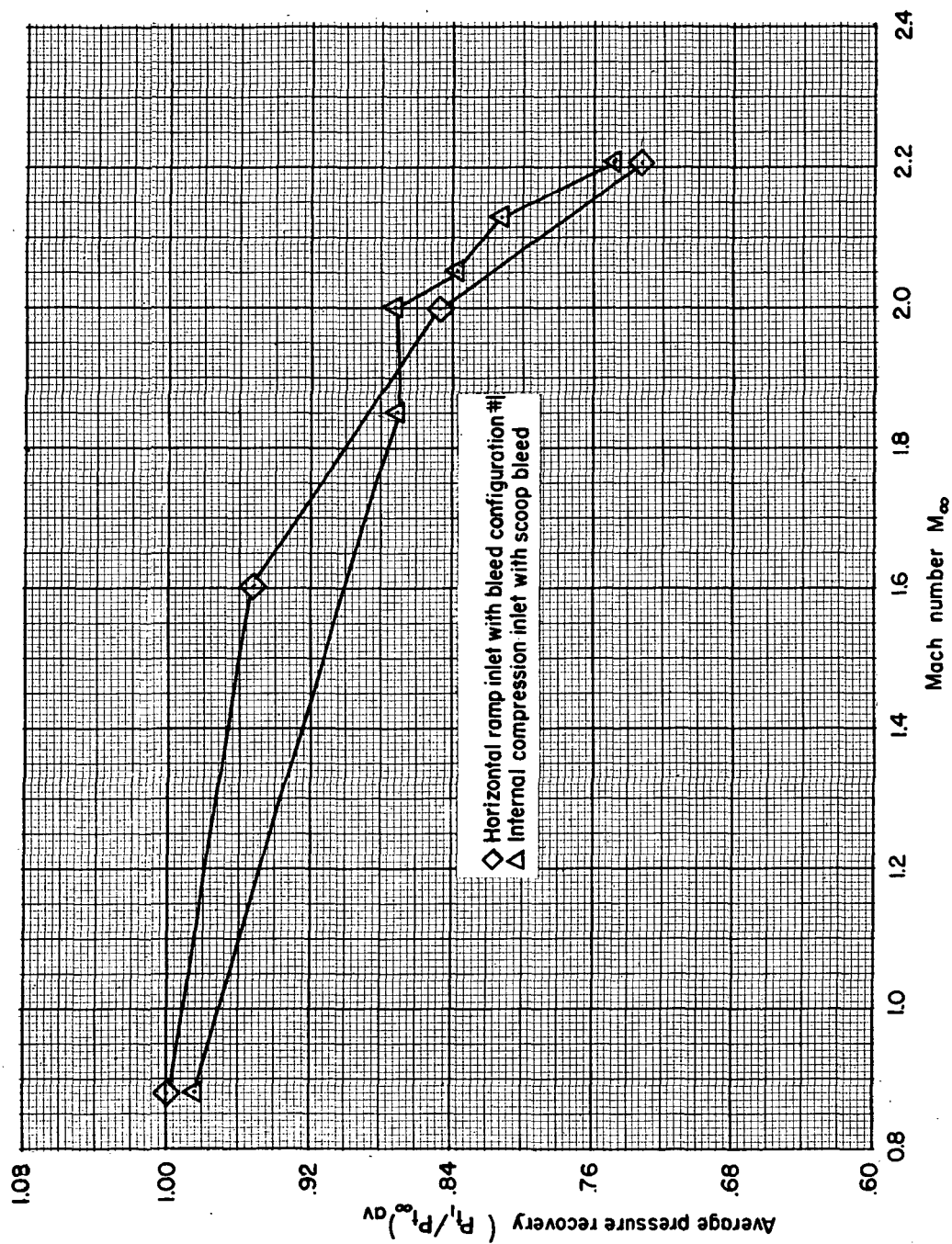
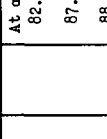
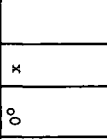
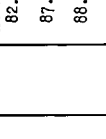
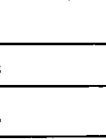
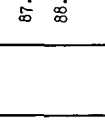
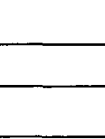
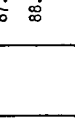
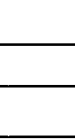


Figure 22.- Off-design pressure recovery at  $\alpha = 2.0^\circ$ .

CONFIDENTIAL

CONFIDENTIAL

NOTES: (1) Reynolds number is based on the diameter of a circle with the same area as that of the capture area of the inlet.  
(2) The symbol \* denotes the occurrence of buzz.

Report and facility	Description		Test parameters				Test data			Performance		Remarks			
			Free-stream Mach number	Reynolds number $\times 10^{-6}$	Angle of attack, deg	Angle of yaw, deg	Inlet-flow profile	Discharge-flow profile	Flow picture	Maximum total-pressure recovery	Mass-flow ratio				
Confidential NASA TM X-107 Ames 6-by 6-ft supersonic W.T.			1	Holes on ramp	2.0	.91	0 - 11°	0°	x			At $\alpha=2^\circ$ 82.6	0.4 to 0.86	A comparison of the performance of three external compression and one internal compression inlet. Each inlet was mounted individually on the side of a common fuselage. The ducting was designed for clustered engine operation.	
			2	Holes on ramp with slotted throat									87.2		0.5 to 1.0
			$\approx 8$	Holes on annulus scoop on centerbody									88.2		0.96
Confidential NASA TM X-107 Ames 6-by 6-ft supersonic W.T.			1	Holes on ramp	2.0	.91	0 - 11°	0°	x			At $\alpha=2^\circ$ 82.6	0.4 to 0.86	A comparison of the performance of three external compression and one internal compression inlet. Each inlet was mounted individually on the side of a common fuselage. The ducting was designed for clustered engine operation.	
			2	Holes on ramp with slotted throat									87.2		0.5 to 1.0
			$\approx 8$	Holes on annulus scoop on centerbody									88.2		0.96
Confidential NASA TM X-107 Ames 6-by 6-ft supersonic W.T.			1	Holes on ramp	2.0	.91	0 - 11°	0°	x			At $\alpha=2^\circ$ 82.6	0.4 to 0.86	A comparison of the performance of three external compression and one internal compression inlet. Each inlet was mounted individually on the side of a common fuselage. The ducting was designed for clustered engine operation.	
			2	Holes on ramp with slotted throat									87.2		0.5 to 1.0
			$\approx 8$	Holes on annulus scoop on centerbody									88.2		0.96
Confidential NASA TM X-107 Ames 6-by 6-ft supersonic W.T.			1	Holes on ramp	2.0	.91	0 - 11°	0°	x			At $\alpha=2^\circ$ 82.6	0.4 to 0.86	A comparison of the performance of three external compression and one internal compression inlet. Each inlet was mounted individually on the side of a common fuselage. The ducting was designed for clustered engine operation.	
			2	Holes on ramp with slotted throat									87.2		0.5 to 1.0
			$\approx 8$	Holes on annulus scoop on centerbody									88.2		0.96

Bibliography

These strips are provided for the convenience of the reader and can be removed from this report to compile a bibliography of NASA inlet reports. This page is being added only to inlet reports and is on a trial basis.

CONFIDENTIAL

~~CONFIDENTIAL~~

~~CONFIDENTIAL~~